# Two-photon blockade and photon-induced tunneling generated by squeezing

Anna Kowalewska-Kudłaszyk,[1] Shilan Ismael Abo,[1,2] Grzegorz Chimczak,[1] Jan Peřina Jr.,[3] Franco Nori,[4,5] and Adam Miranowicz[1,4]

[1]*Faculty of Physics, Adam Mickiewicz University, 61-614 Poznań, Poland*

[2]*Department of Physics, University of Duhok, 1006 AJ Duhok, Kurdistan Region, Iraq*

[3]*Joint Laboratory of Optics, Faculty of Science, Palacký University, 17. listopadu 12, 771 46 Olomouc, Czech Republic*

[4]*RIKEN Center for Emergent Matter Science, Wako, Saitama 351-0198, Japan*

[5]*Department of Physics, University of Michigan, Ann Arbor, Michigan 48109-1040, USA*

(Received 22 August 2019; published 27 November 2019)

Inspired by the recent experiment of Hamsen *et al.* [Phys. Rev. Lett. **118**, 133604 (2017)], which demonstrated two-photon blockade in a driven nonlinear system (composed of a harmonic cavity with a driven atom), we show that two-photon blockade and other nonstandard types of photon blockade and photon-induced tunneling can be generated in a driven harmonic cavity without an atom or any other kind of nonlinearity, but instead coupled to a nonlinear (i.e., squeezed) reservoir. We also simulate these single- and two-photon effects with squeezed coherent states and displaced squeezed thermal states.

DOI: 10.1103/PhysRevA.100.053857

## I. INTRODUCTION

### A. Squeezed states of light

Squeezed states of light [1], which have less quantum noise in one quadrature than a coherent state, are a powerful resource for quantum technologies. These include quantum communication, improving the precision of optical measurements, and fundamental spectroscopic tests of general relativity and quantum mechanics [2–6]. Although squeezed states were already studied in 1927 by Kennard [7] and the squeezing operator was introduced in 1955 [8,9], these states had not been attracting much attention for 50 years. A real practical interest in squeezed states has been triggered only 40 years ago by finding their first applications for detecting gravitational waves via supersensitive interferometry [10–13]. Since the pioneering experimental generation of squeezed states via four-wave mixing in 1985 by Slusher *et al.* [14], shortly followed by two other experiments [15,16], various methods of squeezed-light generation have been implemented experimentally not only for optical fields [6], but also for microwave fields using superconducting quantum circuits [17]. The first long-term practical applications of squeezed-vacuum states were demonstrated in 2013 for increasing the astrophysical limits of gravitational-wave detectors including the laser interferometer gravitational-wave observatory (LIGO) [18] and the gravitational-wave observatory (GEO 600) detectors [19]. Among many applications of squeezing, we mention also recent proposals of an exponential enhancement of light-matter interactions via squeezing [20–25] (for a review see Ref. [26]). Such increased interactions at the single-photon level can fundamentally change nonlinear optical effects, including photon blockade (PB) [27,28]. (This and other abbreviations used in this paper are also defined in Table I.) Here we study multiphoton correlations in squeezed coherent states (SCS), displaced squeezed thermal states (DSTS), and light generated by a driven harmonic cavity coupled to a squeezed reservoir for generating (or simulating) various kinds of PB.

### B. Single-photon blockade

The phenomenon of Coulomb's blockade has its optical analog, known as PB [29] (also referred to as nonlinear quantum scissors [30]). PB (or more precisely single-photon blockade, 1PB) refers to the effect in which a single photon generated in a driven nonlinear system (as those schematically shown in Fig. 1) can block the generation of more photons in the system. This effect was first predicted by Tian and Carmichael [31], Leoński and Tanaś [32], and later by Imamoğlu *et al.* [29], who coined the term *photon blockade* and studied the effect in the steady-state limit. Indeed, Ref. [31] predicted PB by demonstrating a two-state behavior in a driven optical cavity containing one atom, as shown in Fig. 1(b) and discussed in Appendix A, applying the quantum trajectory method to the Jaynes-Cummings model, while Ref. [32] predicted the PB effect in a driven Kerr nonlinear cavity and showed its application for the generation of the single-photon Fock state. Note that the Jaynes-Cummings model in the dispersive limit (i.e., far off resonance) becomes equivalent to the Kerr Hamiltonian, which shows the correspondence of the PB predictions of Refs. [31,32]. We also mention that PB has a mechanical analog referred to as phonon blockade, i.e., blockade of quantum excitations of mechanical oscillators [33–36].

PB has been experimentally generated in a number of driven systems of single [37–44] and two [45,46] resonators with a nonlinearity, as shown schematically in Figs. 1(b) and 1(c), respectively. Such a nonlinearity can be induced by a two-level atom (or atoms) coupled to one or both cavities. In the dispersive regime, such atom-cavity interaction can effectively lead to a Kerr-type nonlinearity as mentioned above. Note that PB can be generated not only in a

 

TABLE I. Abbreviations used in this paper.

| Full Name | Abbreviation |
|---|---|
| Photon blockade | PB |
| Nonstandard photon blockade | NPB |
| Single-photon (two-photon) blockade | 1PB (2PB) |
| Photon-induced tunneling | PIT |
| Two-photon (three-photon) tunneling | 2PT (3PT) |
| Squeezed coherent states | SCS |
| Displaced squeezed thermal states | DSTS |
| Photon antibunching | PAB |

Kerr-nonlinear driven cavity, but also other types of nonlinearities enable the generation of PB. The occurrence of PB is usually experimentally characterized by the second-order correlation function $g^{(2)}(0) < 1$, which means that the PB generated state exhibits the sub-Poissonian photon-number statistics, also referred to as (single-time) photon antibunching (PAB). PB and the generation of Bell states in two-cavity driven nonlinear systems, as shown in Fig. 1(c) and discussed in Appendix A, were first demonstrated in Refs. [47,48]. It was later shown in Refs. [49,50] that the nonlinear system of Fig. 1(c) can exhibit surprisingly strong single-time PAB for weak nonlinearities or, equivalently, weak atom–cavity-field couplings. This effect is now usually referred to as unconventional PB [51].

Note that this single-time PAB should not be confused with standard two-time PAB, defined by $g^{(2)}(\tau) > g^{(2)}(0)$ for small delay times $\tau$, which is another important feature of PB. Indeed, if one considers single-PB as a true source of single photons, one would be required to satisfy not only single-time PAB, but also two-time PAB, characterized by a local minimum of the second-order correlation function,

$$g^{(2)}(\tau) = \lim_{t\to\infty} \frac{\langle \hat{a}^\dagger(t)\hat{a}^\dagger(t+\tau)\hat{a}(t+\tau)\hat{a}(t)\rangle}{\langle \hat{a}^\dagger(t)\hat{a}(t)\rangle\langle \hat{a}^\dagger(t+\tau)\hat{a}(t+\tau)\rangle}, \qquad (1)$$

as a function of the delay time $\tau \approx 0$, where $\hat{a}$ ($\hat{a}^\dagger$) is the annihilation (creation) operator of an optical mode. Thus, at least the following conditions should be satisfied for "true" single-PB:

$$g^{(2)}(0) < 1 \quad \text{and} \quad g^{(2)}(0) < g^{(2)}(\tau), \qquad (2)$$

for small $\tau$. For brevity, we analyze two-time PAB only in Sec. III and Fig. 2. Otherwise we limit our characterization of PB to single-time correlation functions.

### C. Multiphoton blockade

Single-PB has been generalized to include two-PB and multi-PB effects [52–61]. Two-PB was first experimentally demonstrated by Hamsen *et al.* in 2017 [44]. We also note earlier theoretical works on multi-PB in dissipation-free driven Kerr systems [62,63] (for reviews see Refs. [30,64]). Multi-*phonon* blockade, which is a mechanical analog of multi-PB, was studied in Ref. [35]. Multi-PB in dissipation-free

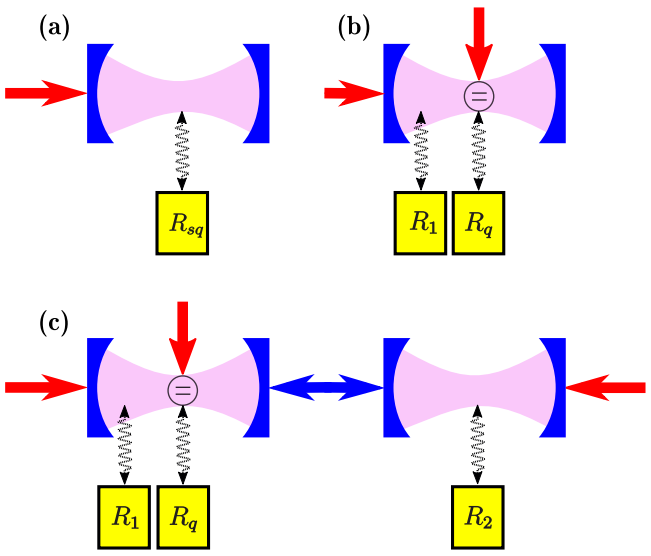


FIG. 1. Schematics of three prototype systems for observing photon blockade and photon-induced tunneling. (a) An unusual photon blockade device, described in Sec. III A, which is composed of a driven harmonic cavity coupled to a quantum (squeezed) reservoir $R_{sq}$. Panel (a) is shown in contrast to the common photon blockade devices (see Appendix A for more details). (b) A driven anharmonic cavity (due to the atom) coupled to a harmonic reservoir $R_1$. (c) A two-cavity system, which is the anharmonic resonator shown in panel (b) coupled to a harmonic (or anharmonic) resonator linked to a harmonic reservoir $R_2$. The anharmonicity can be induced in a harmonic resonator by its coupling to a two-level atom (qubit) as shown in panels (b) and (c). This qubit is coupled to a reservoir $R_q$. Red arrows denote classical coherent drives applied to a cavity or a qubit. Note that in setup (a) the cavity anharmonicity is replaced by the reservoir anharmonicity.

systems enables generation of quantum optical states in a finite-dimensional Hilbert space including finite-dimensional analogs of coherent and squeezed states of light [62,64–67].

Intuitively, two-PB (and analogously multi-PB) occurs if the single- and two-photon Fock states, which are generated in a driven nonlinear system, block the generation of more photons in the system. This paper is focused on the *study of two-PB and other kinds of single- and two-photon correlations.*

For any classical states, the second-order equal-time correlation function satisfies $g^{(2)}(0) \geqslant 1$, which is a property of classical intensity fluctuations. The states for which $g^{(2)}(0) < 1$ have the sub-Poissonian photon-number statistics and, thus, are *nonclassical* (see Appendix C). This condition is also used for identifying the presence of single-photon blockade (1PB). The analysis of higher-order correlations is necessary to characterize multi-PB or other types of nonstandard PB (NPB).

Thus, in our study of multi-PB, we apply the $k$th-order equal-time correlation functions, $g^{(k)}(0) = \langle(\hat{a}^\dagger)^k\hat{a}^k\rangle/\langle\hat{a}^\dagger\hat{a}\rangle^k$, describing the probability of measuring simultaneously $k$ photons. In PB experiments, the second-order correlation functions $g^{(2)}(0)$ and $g^{(2)}(\tau)$ are usually measured, except the experiment of Hamsen *et al.* [44], where also the third-order correlation functions $g^{(3)}(0)$ and $g^{(3)}(\tau)$ were measured to confirm two-PB.

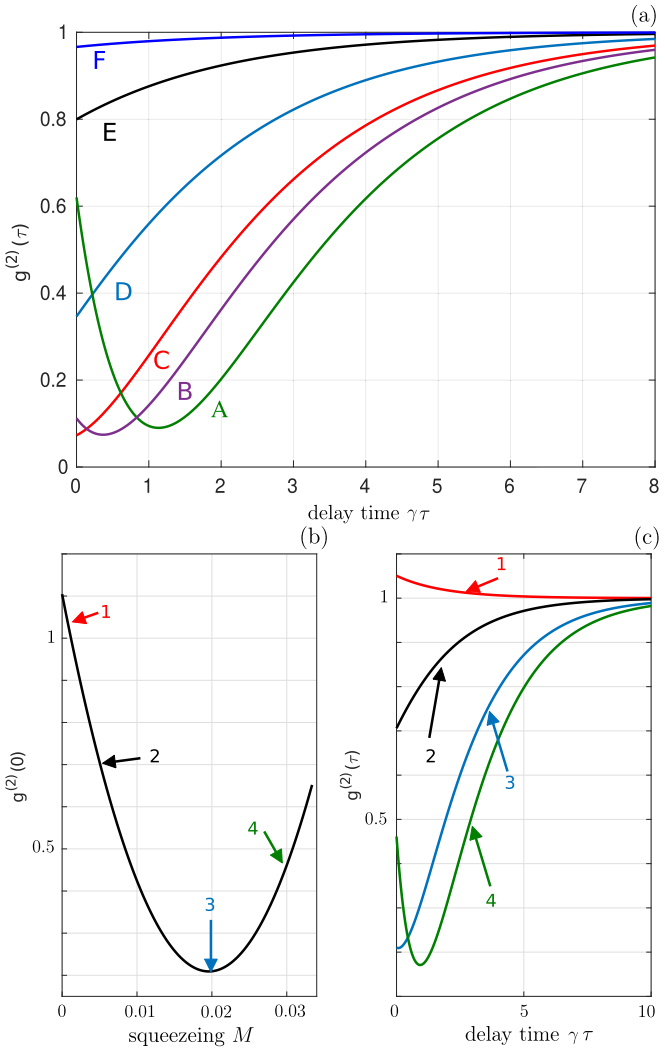


FIG. 2. Squeezed-reservoir model: steady-state second-order correlation function $g^{(2)}(\tau)$ vs (a), (c) the (rescaled) delay time $\gamma\tau$ between the measurements of subsequent photons and (b) the reservoir squeezing parameter $M$ for various values of the external field strength $\varepsilon$ at the resonance, $\Delta = 0$, between the cavity and driving fields, with the damping rate $\gamma = 1$. Moreover, in panel (a) we set $\varepsilon/\gamma$ =0.05 (curve A), 0.06 (B), 0.07 (C), 0.1 (D), 0.2 (E), and 0.5 (F), and assume that the reservoir is maximally squeezed with the reservoir mean photon number $n = 0.003$, which corresponds to $M = 0.017$. The $\tau$ dependences for the four specific points in panel (b) are shown in panel (c). In panels (b) and (c) we set $\varepsilon/\gamma = 0.07$ and $n = 0.001$. It is evident that the curves 2 and 3 (1 and 4) show two-time photon antibunching (bunching) in panel (c). This implies that only the points 2 and 3 in panel (b) can correspond to "true" single-photon blockade states.

We note that experimental tests of PB are not limited to measuring $g^{(k)}(0)$ and $g^{(k)}(\tau)$. Indeed, the occurrence of PB can also be revealed by showing, e.g., a staircase dependence of the total transmitted power through a driven nonlinear system for different incident photon bandwidths, which was experimentally demonstrated by Hoffman *et al.* [40] or a staircase dependence of the mean photon number in the ground state of a given Kerr nonlinear system on a rescaled detuning [68]. Such dependences are photonic analogs of a Coulomb-blockade staircase. This paper is focused on characterizing multi-PB via $g^{(k)}(0)$ and $g^{(2)}(\tau)$ only.

TABLE II. Different types of photon blockade and photon tunneling classified via $g^{(2)}(0)$ and $g^{(3)}(0)$. Four of these types of photon-number correlations can be exhibited by the steady-state light generated by the squeezed-reservoir system, as well as squeezed coherent states and displaced squeezed thermal states, which are shown in Figs. 3–5, respectively.

| Case | Permutation | Inequalities | Effect |
|---|---|---|---|
| a | (1 2 3) | $1 < g^{(2)}(0) < g^{(3)}(0)$ | 3PT |
| b | (1 3 2) | $1 < g^{(3)}(0) < g^{(2)}(0)$ | 2PT |
| c | (2 1 3) | $g^{(2)}(0) < 1 < g^{(3)}(0)$ | 1PB (type 2) |
| d | (2 3 1) | $g^{(2)}(0) < g^{(3)}(0) < 1$ | 1PB (type 3) |
| e | (3 1 2) | $g^{(3)}(0) < 1 < g^{(2)}(0)$ | 2PB and 2PT |
| f | (3 2 1) | $g^{(3)}(0) < g^{(2)}(0) < 1$ | 1PB (type 1) |

### D. Photon-induced tunneling

Photon-induced tunneling (PIT) refers to a photon-number correlation effect, which *enhances* the probability of subsequent photons (from a coherent drive) to enter the driven cavity [38,60,61,69–73]. Evidently, this process is inverse to PB, in which the probability that the subsequent photons of a drive enter the driven cavity is *decreased* (or even essentially vanishing). PIT has been observed experimentally in Refs. [38,69,72].

Standard two-photon tunneling (two-PT), where the simultaneous arrival of two photons is enhanced compared to single-photon arrivals, is usually characterized by the super-Poissonian photon-number statistics (i.e., single-time photon bunching), when $1 < g^{(2)}(0)$ [69–71]. Analogously, standard three-photon tunneling (three-PT) is a photon-number correlation effect, in which the simultaneous arrival of three photons is enhanced compared to the two-photon and single-photon arrivals. Thus, three-PT can be characterized by the conditions [60,71]

$$1 < g^{(2)}(0) < g^{(3)}(0). \tag{3}$$

Note that other definitions of PIT are used in the literature (see Ref. [60] for a comparison), e.g., those based on a local maximum of $g^{(2)}(\tau)$ at $\tau = 0$ (i.e., corresponding to two-time photon bunching) [38] or the requirement that $g^{(3)}(0) > g^{(2)}(0)$, i.e., the simultaneous arrival of three photons is enhanced compared to the simultaneous two-photon arrivals [72] without specifying whether $g^{(2)}(0)$ exhibits the super- or sub-Poissonian statistics. Various types of PIT in comparison to PB are listed in Table II.

### E. Photon blockade and photon-induced tunneling via squeezing

It is known that SCS can exhibit the (second-order) sub-Poissonian photon-number statistics (also referred to as single-time PAB). This effect is also an important feature of light generated via photon blockade.

The vast majority of previous works on PB assumed that dissipation of a PB system can be modeled via its linear

coupling to a harmonic reservoir (a thermal bath). Only a few works, including Refs. [74,75], were analyzing PB in systems coupled to nonlinear reservoirs. In such dissipative systems, PB can result from (i) a system nonlinearity, (ii) a reservoir nonlinearity, or (iii) both of them. Single- and multi-PB effects in a Kerr-nonlinear system coupled to a nonlinear (squeezed) reservoir were analyzed in Ref. [74]. Shortly after that publication, a single-PB effect generated solely by a nonlinear (squeezed) reservoir was studied in a linear system in Ref. [75]. Here we analyze various PB effects and PIT in a harmonic cavity coupled to squeezed systems, as shown in Fig. 1(a). The other two common systems, which enable the generation of conventional and unconventional PB, are schematically shown in Figs. 1(b) and 1(c), respectively. Note that some other schemes for PB can be obtained by combining the three schemes shown in this figure.

The main objective of this paper is to analyze whether squeezing plays an important role in generating various types of PB (especially multiphoton effects). In other words, we address the question whether PB can be observed in a driven harmonic resonator without a strongly nonlinear medium [like in the standard PB setup shown in Fig. 1(b)] and without relying on multipath interference, as in the PB setup shown in Fig. 1(c).

The paper is organized as follows. In Sec. II, we specify the criteria of multi-PB and PIT. In Sec. III, we numerically show that a two-photon decay process of light generated in an optically linear system (a harmonic resonator) can induce two-PB. Then, in Sec. IV, we analytically study the relations between $g^{(2)}(0)$ and the higher-order correlation functions $g^{(k)}(0)$ for the squeezed coherent states and the displaced squeezed thermal states, to demonstrate more explicitly the possibility of generating two-PB, three-PT, and various types of nonstandard single-PB via squeezing. The question of nonclassicality of the studied effects and states is addressed in Sec. V and Appendices C–E. We also compare the proposed method for generating multi-PB with the standard PB setups in Appendix A. Moreover, for pedagogical reasons, we present more details about the master equation for a squeezed reservoir and recall its relation to the standard master equation in Appendix B. We conclude in Sec. VI.

In the main paper, we use several abbreviations. We concisely list them in Table I to facilitate the following exposition.

## II. CRITERIA FOR VARIOUS TYPES OF PHOTON BLOCKADE

### A. Refined criteria for multiphoton blockade

The mechanisms of both conventional and unconventional single-PB under proper resonance conditions can be generalized to generate also two- and multi-PB, i.e., the generation of two or a larger number of photons at the same instance of time.

Intuitively, $k$-PB can be understood as the generation of a state $\hat{\rho}$ satisfying the conditions for the photon-number probabilities $P_k = \langle k|\hat{\rho}|k\rangle$ as follows [44,53]:

$$P_{k+1} \approx 0 \quad \text{and} \quad P_k \gg P_{k+1}. \tag{4}$$

However, in more realistic scenarios, the conditions in Eq. (4) are replaced by weaker criteria, where the photon-number distribution $P_k$ of $\hat{\rho}$ is compared with the Poissonian distribution $P_k^{\mathrm{CS}}$, describing the photon-number statistics of a coherent state. Specifically,

$$P_{k+1} < P_{k+1}^{\mathrm{CS}} \quad \text{and} \quad P_k \geqslant P_k^{\mathrm{CS}}, \tag{5}$$

where the probability $P_k^{\mathrm{CS}} = |\langle\alpha|k\rangle|^2$ is for a coherent state $\alpha$ with the same mean photon number as that for $\hat{\rho}$, i.e., $\langle\alpha|\hat{n}|\alpha\rangle = |\alpha|^2 = \mathrm{Tr}(\hat{\rho}\hat{n})$, where $\hat{n} = \hat{a}^\dagger\hat{a}$ is the photon-number operator. The conditions for the probabilities $P_k$ can be replaced by those based on the experimentally accessible $k$th-order correlation function,

$$g^{(k)}(0) = \frac{\langle(\hat{a}^\dagger)^k\hat{a}^k\rangle}{\langle\hat{n}\rangle^k} = \frac{\langle\hat{n}^{[k]}\rangle}{\langle\hat{n}\rangle^k} = \frac{\sum_{n=0}^{\infty} P_n n^{[k]}}{\langle\hat{n}\rangle^k}, \tag{6}$$

where, as usual, $\hat{a}$ ($\hat{a}^\dagger$) is the annihilation (creation) operator, $\langle\hat{n}^{[k]}\rangle = \langle(\hat{a}^\dagger)^k\hat{a}^k\rangle$, and $n^{[k]} = n(n-1)\cdots(n-k+1)$ is the factorial power (also called the falling power). Thus, the criteria for PB given in Eq. (4) can be replaced by

$$g^{(k+1)}(0) \approx 0 \quad \text{and} \quad g^{(k)}(0) \gg g^{(k+1)}(0). \tag{7}$$

In this paper, we assume that $k$-PB is defined by the following two criteria derived by Hamsen *et al.* [44]:

$$\begin{aligned} &\text{Criterion 1}: \quad g^{(k+1)}(0) < A \equiv \exp(-\langle\hat{n}\rangle); \\ &\text{Criterion 2}: \quad g^{(k)}(0) \geqslant B^{(k)} \equiv A + \langle\hat{n}\rangle g^{(k+1)}(0), \end{aligned} \tag{8}$$

which replace the criteria in Eq. (5).

We note that the definition of multi-PB in Eq. (8) has some drawbacks and limitations. Strictly speaking, the criteria in Eq. (8) can only be considered a PB witness, i.e., necessary but not sufficient conditions of PB. Note that second-order single-time photon antibunching [$g^{(2)}(0) < 1$] is the most common test of single-PB, but it is also only a necessary but not sufficient condition for PB. An intuitive "orthodox" interpretation of single- and multi-PB effects can be given as follows: $k$-PB ($k = 1, 2, ...$) corresponds to the effect, in which the photon occupation of the first $k$ energy levels of a driven nonlinear system blocks the generation of more photons in the system. In other words, $k$-PB corresponds to an effective truncation of the Hilbert space spanning a given state at the $k$-photon Fock state $|k\rangle$ so the contributions of the Fock states $|k+l\rangle$ for $l > 0$ can be effectively ignored, which means that $\langle k|\hat{\rho}|k\rangle \gg \langle k+l|\hat{\rho}|k+l\rangle$ or, alternatively, $g^{(k)}(0) \gg g^{(k+l)}(0)$, for any $l > 0$. However, the above conditions are usually only checked for $l = 1$, ignoring the analysis of the cases for $l > 1$. Such objection also applies to many studies of single-PB based on requiring $g^{(2)}(0) < 1$ and ignoring the values of $g^{(3)}(0)$ and higher-order correlation functions.

### B. Simplified criteria for multiphoton blockade

Note that if $\langle\hat{n}\rangle \ll 1$ then the refined conditions for multi-PB, given in Eq. (8), simplify to the following familiar criteria for $\hat{\rho}$:

$$g^{(k+1)}(0) < 1 \quad \text{and} \quad g^{(k)}(0) \geqslant 1, \tag{9}$$

which mean that, in this small photon-number limit, the state generated via $k$-PB exhibits (single-time) $(k+1)$-PAB, and

$k$-photon bunching if $g^{(k)}(0) > 1$ or the so-called unbunching if $g^{(k)}(0) = 1$.

Thus, two-photon and three-PB effects can be given by the following relations for the correlation functions:

$$g^{(2)}(0) \geqslant 1 \quad \text{and} \quad g^{(3)}(0) < 1; \tag{10}$$

$$g^{(2)}(0), g^{(3)}(0) \geqslant 1 \quad \text{and} \quad g^{(4)}(0) < 1, \tag{11}$$

respectively. Note that we have added an extra condition for $g^{(2)}(0)$ in Eq. (11), which is not required in the criteria specified in Eqs. (8) and (9). Moreover, in this simplified characterization of PB we ignore the requirements on two-time correlation functions $g^{(k)}(\tau)$, including $g^{(2)}(\tau)$.

Thus, in the case of two-PB, the three-photon probability has to be suppressed and simultaneously the probability of observing two photons should be enhanced. Analogously, the suppression of the four-photon probability and the increase in the probabilities of a lower number of photons would lead to three-PB.

Both types of PB, which are characterized by the simplified and refined criteria, correspond to nonclassical effects, because they require the sub-Poissonian photon-number statistics (of any given order $k$), as described in greater detail in Appendix C.

As mentioned above, the refined criteria in Eq. (8) reduce to the conditions in Eq. (10) for small photon numbers $\langle\hat{n}\rangle \ll 1$. But, in principle, these simplified criteria can be applied even if $\langle\hat{n}\rangle > 1$, but then the predicted PB can differ from that based on the refined criteria in Eq. (8). It might also be the case that a given state exhibits, e.g., two-PB according to the refined criteria, but not according to the simplified criteria. Actually, we will show such cases in the following sections.

Now, we consider a simple example of such different predictions of two-PB according to Eqs. (8) and (9). Specifically, the two-photon Fock state $|2\rangle$, for which $g^{(2)}(0) = 1/2$ and $g^{(3)}(0) = 0$, can be considered a two-PB state according to the refined criteria in Eq. (8), because $g^{(2)}(0) > \exp(-2) \approx 0.135$ and $g^{(3)}(0) < \exp(-2)$. Note that the simplified criteria in Eq. (9) can, in principle, be applied to the two-photon Fock state $|2\rangle$. However, since $A \equiv \exp(-\langle\hat{n}\rangle)$ is not negligible, the predictions of PB for $|2\rangle$ according to the refined and simplified criteria are different. Indeed, the Fock state $|2\rangle$ is not considered a two-PB state according to the simplified criteria (9).

### C. Nonstandard types of photon blockade

As described in previous subsections, the simplified condition for observing single PB corresponds to the requirement of single-time PAB. If the following additional condition $g^{(3)}(0) < g^{(2)}(0)$ is satisfied, as desirable for good single-photon sources, then we refer to this effect as single-PB of type 1, which is characterized by

$$g^{(3)}(0) < g^{(2)}(0) < 1. \tag{12}$$

Apart from this single-PB, there are other possibilities of obtaining quantum photon-number statistics by specifying the relations between higher-order single-time correlations $g^{(k)}(0)$ and/or the second-order two-time correlations $g^{(2)}(\tau)$. These include the following types of PB.

(1) We recall that, in order to consider single-PB as a true source of single photons, the generated light via PB should also exhibit two-time PAB as given in Eq. (2). Indeed, it is known that the sub-Poissonian photon-number statistics (i.e., single-time PAB) of a field can be accompanied with both two-time PAB and two-time photon bunching, and vice versa (see, e.g., Ref. [76] and references therein). Thus, if light exhibits single-time PAB and two-time photon bunching [i.e., a local maximum of $g^{(2)}(\tau)$ for small $\tau$], one can refer to it as nonstandard single-PB , because it is *not* characterized by Eq. (2). Examples of this nonstandard PB are analyzed in Sec. III and shown in Fig. 2. In the following we mainly analyze other types on nonstandard PB based solely on single-time correlation functions.

(2) In greater detail we analyze a special kind of nonstandard PB characterized by the single-time correlation functions satisfying the conditions

$$g^{(2)}(0) < 1 < g^{(3)}(0), \tag{13}$$

which was first studied in greater detail in Ref. [77] under the name *unconventional PB*. However, in order to avoid confusion of this type of PB and unconventional PB studied in Refs. [45,46,51], we refer to the effect characterized by Eq. (13) as nonstandard PB of type 2.

It is seen that this nonstandard PB occurs when the probability of measuring two photons at the same time is suppressed and, simultaneously, the probability of obtaining three photons is enhanced. Note that this effect can be generated by different physical mechanisms in different systems: (i) by using large nonlinearities in conventional PB systems, as shown in Fig. 1(b); (ii) by small nonlinearities and multipath interference in unconventional PB systems, as shown in Fig. 1(c); or (iii) by exploiting squeezing in, e.g., linear systems coupled to a squeezed reservoir, as shown in Fig. 1(a) and studied here.

(3) One can modify the condition for $g^{(3)}(0)$ in Eq. (13) to consider another type (say type 3) of single-PB, as characterized by

$$g^{(2)}(0) < g^{(3)}(0) < 1. \tag{14}$$

The latter two types of nonstandard single-PB are listed in Table II and a few examples of such effects generated via squeezing are discussed in the following sections and shown in Figs. 3–6.

Note that we found examples of nonstandard PB concerning unusual properties of both single- and two-time correlation functions. But, for brevity, we do not present such examples here.

We also note that nonclassical states often satisfy the conditions $g^{(2)} < g^{(3)} < \ldots < g^{(k)} < 1$, as those studied in Refs. [78,79], where the sub-Poissonian statistics was resulting from postselection. Such states can also be used for simulating nonstandard single-PB effects.

## III. VARIOUS TYPES OF PHOTON BLOCKADE AND TUNNELING GENERATED BY A SQUEEZED RESERVOIR

### A. Model

Here we will show that a squeezed reservoir can induce various types of PB and PIT, including two-photon effects in a driven *harmonic* resonator.

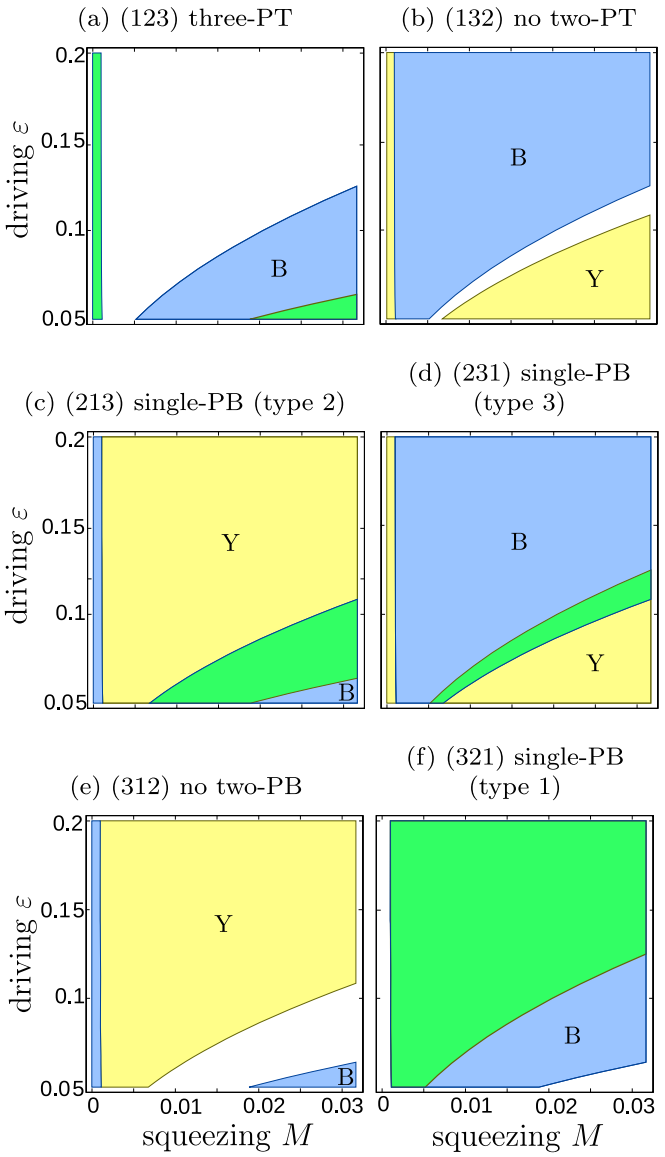


FIG. 3. Squeezed-reservoir model: photon-number correlations of light generated in a driven harmonic cavity coupled to a squeezed reservoir, assuming $n = 0.01$ and $\Delta = 0$. The regions of the driving strength $\varepsilon$ and the reservoir squeezing parameter $M$ satisfying the six conditions, which are listed in Table II for the correlation functions $g^{(2)}(0)$ and $g^{(3)}(0)$, are shown here in yellow (Y) and blue (B), respectively. The regions in green show the ranges of the parameters $M$ and $\varepsilon$ for which given criteria are satisfied simultaneously by $g^{(2)}(0)$ and $g^{(3)}(0)$ indicating a specific type of photon blockade or photon-induced tunneling. In grayscale, yellow is the brightest, and green looks slightly darker than blue. Yellow is also indicated by "Y," and blue is indicated by "B."

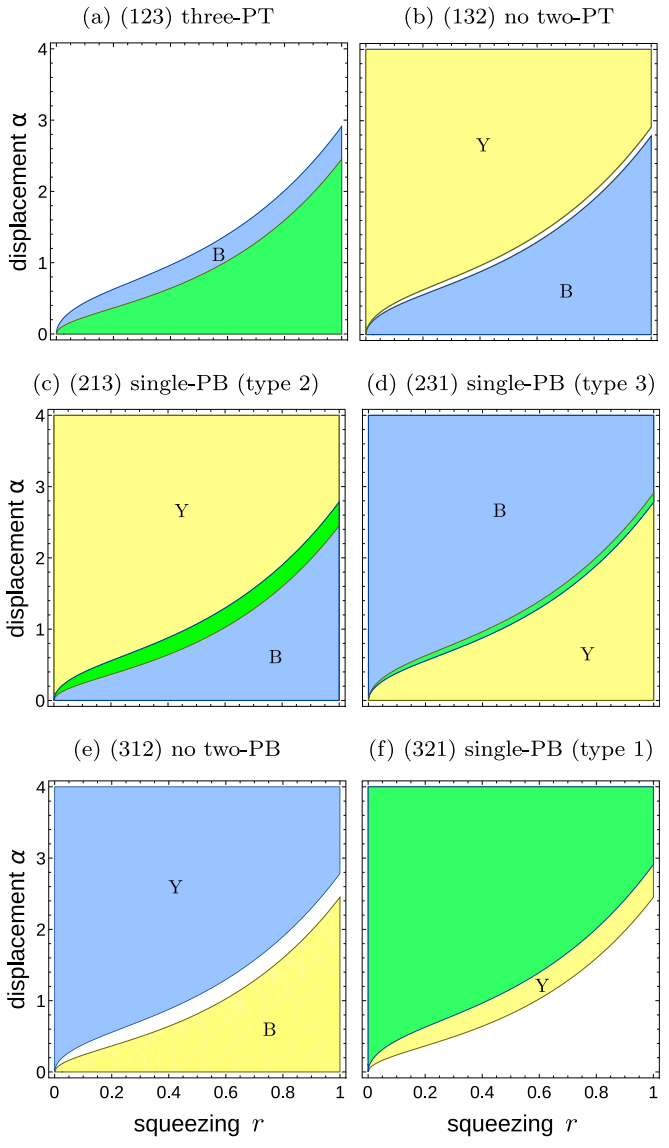


FIG. 4. Photon-number correlations in the squeezed coherent states showing the regions of the displacement ($\alpha$) and squeezing ($r$) parameters for which the conditions in Table II are satisfied. This figure uses the same notation and coloring, and carries a similar message as in Fig. 3. For example, the green region in figure (c) (213) shows the ranges of parameters for which the conditions $g^{(2)}(0) < 1 < g^{(3)}(0)$ are satisfied, as in Table II (c). The yellow (blue) region shows the parameter ranges satisfying solely the condition $g^{(2)}(0) < 1$ [$g^{(3)}(0) > 1$]. Yellow (blue) is also indicated by "Y" ("B").

Specifically, as an example of a physical system, in which squeezing interactions induce PB, we use a single optical cavity of a frequency $\omega_c$, which is externally driven by a laser field of an amplitude $\varepsilon$ with a frequency $\omega_d$. The cavity decays into a squeezed reservoir characterized by the reservoir squeezing parameter $M$. The model is presented in Fig. 1(a). We will show that for such a linear optical system the two-photon dissipation process plays a crucial role in obtaining single- and two-PB, as well as other nonstandard types of nonclassical photon correlations.

The Hamiltonian of the system has the following form (hereafter we set $\hbar = 1$):

$$\hat{H}' = \omega_c \hat{a}^\dagger \hat{a} + \varepsilon(\hat{a}e^{i\omega_d t} + \hat{a}^\dagger e^{-i\omega_d t}). \tag{15}$$

After its transformation to the interaction picture to the frame rotating with the driving frequency $\omega_d$, one obtains the following effective Hamiltonian of the system:

$$\hat{H} = \Delta \hat{a}^\dagger \hat{a} + \varepsilon(\hat{a}^\dagger + \hat{a}), \tag{16}$$

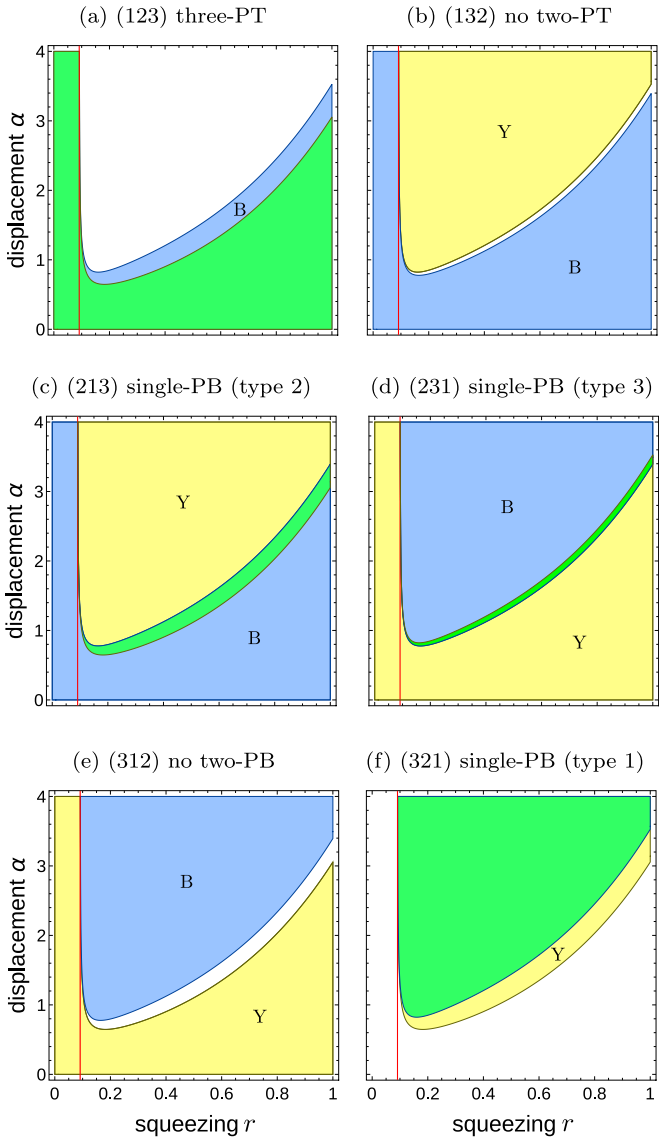


FIG. 5. Photon-number correlations in the displaced squeezed thermal states satisfying the inequalities in Table II, the same as in Fig. 4 but for the states defined in Eq. (23) with $n_{\rm th} = 0.1$. The parameter region on the left-hand (right-hand) side of the red vertical line in all the plots corresponds to the classical (nonclassical) regimes of the states. This red line is plotted at the critical squeezing parameter $r_0 = 0.0912$, which is shown later in Fig. 12 by the solid curve for $n_{\rm th} = 0.1$ for the vanishing entanglement potential, EP = 0.

where $\Delta = \omega_c - \omega_d$ is the detuning between the cavity and driving frequencies.

The evolution of the driven cavity interacting with a squeezed reservoir is governed by the following master equation [80–82]:

$$\frac{d\hat{\rho}}{dt} = -i[\hat{H}, \hat{\rho}] + \frac{1}{2}\gamma(n+1)(2\hat{a}\hat{\rho}\hat{a}^\dagger - \hat{a}^\dagger\hat{a}\hat{\rho} - \hat{\rho}\hat{a}^\dagger\hat{a}) + \frac{1}{2}\gamma n(2\hat{a}^\dagger\hat{\rho}\hat{a} - \hat{a}\hat{a}^\dagger\hat{\rho} - \hat{\rho}\hat{a}\hat{a}^\dagger) - \frac{1}{2}\gamma M(2\hat{a}\hat{\rho}\hat{a} - \hat{a}\hat{a}\hat{\rho} - \hat{\rho}\hat{a}\hat{a}) - \frac{1}{2}\gamma M^\star(2\hat{a}^\dagger\hat{\rho}\hat{a}^\dagger - \hat{a}^\dagger\hat{a}^\dagger\hat{\rho} - \hat{\rho}\hat{a}^\dagger\hat{a}^\dagger). \quad (17)$$

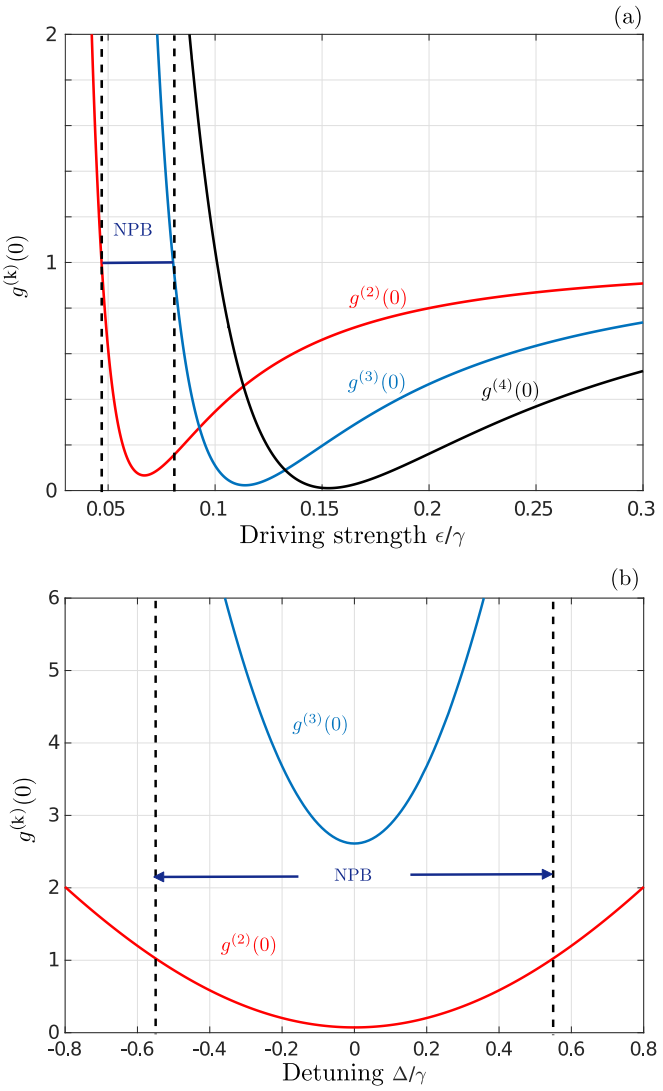


FIG. 6. Squeezed-reservoir model: correlation functions $g^{(k)}(0)$ vs (a) the driving strength $\varepsilon$ for fixed $\Delta = 0$ and (b) the detuning $\Delta$ for the maximally squeezed reservoir for $n = 3 \times 10^{-4}$, which corresponds to $M = 0.017$, for fixed $\varepsilon = 0.07\gamma$. All the parameters are scaled in $\gamma$ units. The regions between the broken lines correspond to nonstandard single-photon blockade (type 2).

We refer to $M$ as a reservoir squeezing parameter and to $n$ as the mean number of reservoir photons. These parameters satisfy the inequality $|M| \leqslant \sqrt{n(n+1)}$. For the squeezed-vacuum reservoir, these parameters are given by $n = \sinh^2(r)$ and $M = \cosh(r)\sinh(r)\exp(-i\theta)$, implying the equality $|M| = \sqrt{n(n+1)}$, where $r$ and $\theta$ correspond, respectively, to the amplitude and phase of the squeezing parameter $\xi = r\exp(i\theta)$ (see Appendix B for more details). Apart from the standard parts in Eq. (17), which describe a thermal-like Markovian reservoir with the mean photon number $n$ allowing for single-photon dissipation, this master equation includes also two-photon decay processes. Indeed, Eq. (17) reduces to the standard master equation for the thermal reservoir by setting $M \to 0$ and $n \to n_{\rm th} = \{\exp[\hbar\omega/(k_B T)] - 1\}^{-1}$, which becomes the mean number of thermal photons at the frequency $\omega$ and temperature $T$, where $k_B$ is the Boltzmann constant.

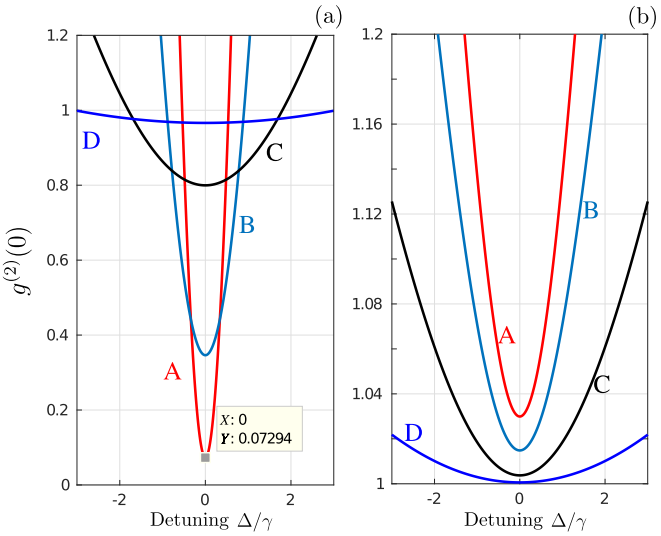


FIG. 7. Squeezed-reservoir model: single-photon blockade in a driven harmonic resonator coupled to a squeezed reservoir. Specifically, the steady-state second-order correlation function $g^{(2)}(0)$ vs the detuning $\Delta$ between the cavity and driving frequencies for various values of the external field strength $\varepsilon$, assuming (a) the squeezed-vacuum reservoir (see Appendix B) with $M = \sqrt{n(n+1)}$ and (b) no squeezing ($M = 0$) of the reservoir. We set the reservoir mean photon number as $n = 3 \times 10^{-4}$, and $\varepsilon/\gamma = 0.07$ (curve A), 0.1 (B), 0.2 (C), and 0.5 (D). All the parameters are scaled in $\gamma = 1$ units. Panel (a) shows strong single-time photon antibunching, especially for $\varepsilon = 0.07\gamma$ and $\Delta = 0$, which characterizes single-photon blockade. Panel (b) shows single-time photon bunching, which confirms that the single-photon blockade in panel (a) results from the squeezed reservoir.

### B. Standard single-photon blockade

As mentioned above, the standard indicator of single-PB is the condition $g^{(2)}(0) < 1$ showing the decreased probability of measuring simultaneously two photons during the process of the cavity-field dissipation.

In Figs. 7(a) and 7(b), we have shown the dependence of single-time steady-state second-order correlation function $g^{(2)}(0)$ versus the detuning $\Delta$ for the harmonic cavity field decaying, respectively, into (a) the squeezed-vacuum reservoir [i.e., the maximally squeezed reservoir with $M = \sqrt{n(n+1)}$] and (b) the standard thermal reservoir ($M = 0$) with the same mean number $n = 0.003$ of reservoir photons. Various external-driving-field strengths are considered. Our first conclusion is that the squeezing of the field in the reservoir is responsible for generating single-PB of the linear-cavity field, as described by the sub-Poissonian photon-number statistics shown in Fig. 7(a), while the interaction with the thermal field of the environment inevitably leads to the super-Poissonian photon-number statistics of the cavity field shown in Fig. 7(b). This effect can be interpreted as PIT. In all of these cases, by tuning the frequency of the external excitation with the cavity frequency, one can assure the lowest possible value of $g^{(2)}(0)$. Additionally, a weaker external driving is preferable to obtain lower values of $g^{(2)}(0)$. For the parameters presented in Fig. 7(a), the lowest value of $g^{(2)}(0)$ is 0.0729. By decreasing the mean photon number inside the squeezed reservoir, or by applying a weaker external field, one can obtain even smaller values of $g^{(2)}(0)$ under the exact resonance condition $\Delta = 0$.

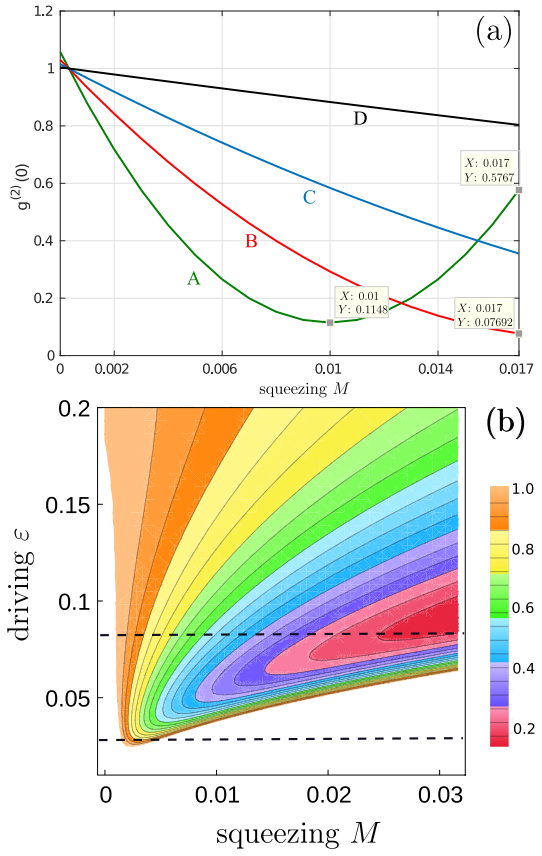


FIG. 8. Squeezed-reservoir model: steady-state correlation function $g^{(2)}(0)$ vs the reservoir squeezing parameter $M$ and the driving strength $\varepsilon$ in a driven harmonic resonator coupled to a squeezed reservoir. We set $\varepsilon/\gamma = 0.05$ (curve A), 0.07 (B), 0.1 (C), and 0.2 (D). Moreover, we assume resonance between the cavity and external fields, $\Delta = 0$, and the mean photon number of the squeezed reservoir is $n = 3 \times 10^{-4}$. All the parameters are scaled in $\gamma$ units. It is seen that, usually, a larger reservoir squeezing parameter $M$ implies stronger single-time PAB, reaching the smallest value of $g^{(2)}(0)$ for the squeezed-vacuum reservoir with $M = \sqrt{n(n+1)}$ (see Appendix B). However, this is not the case for, e.g., $\varepsilon = 0.05\gamma$ in panel (a), when there is an optimal value of $M \ll \sqrt{n(n+1)}$, which results in the strongest single-time PAB. The same surprising result is shown in panel (b) in the area between the dashed lines indicating the range of the external field strength $\varepsilon$ for which $g^{(2)}(0)$ has a minimum for $M < \sqrt{n(n+1)}$.

Figures 8(a) and 8(b) show the dependence of the steady-state single-time second-order correlation $g^{(2)}(0)$ on the reservoir squeezing parameter $M$ and the driving strength $\varepsilon$. Usually, the minimal possible values of $g^{(2)}(0)$ are obtained when the field inside the reservoir is maximally squeezed, i.e., for the squeezed-vacuum reservoir satisfying $M = \sqrt{n(n+1)}$. However, for very weak excitations, the dependence $g^{(2)}(0)$ versus $M$ has a minimum for $M < \sqrt{n(n+1)}$. Thus, it is worth stressing that it is possible to use a nonmaximally squeezed reservoir, which still enables strong single-time PAB for very weak excitations, as shown in Fig. 8(a).

### C. Nonstandard single-photon blockade with two-time photon bunching

Here we discuss whether a squeezed reservoir can generate nonstandard PB exhibiting two-time photon bunching, and single-time PAB. Three examples of this type of PB are shown in Figs. 2(a) and 2(c) by the curves marked as A, B, and 4. These examples should be compared with the examples of true single-PB indicated there by arrows 2 and 3.

More specifically, in Fig. 2(a), the steady-state two-time second-order correlation function $g^{(2)}(\tau)$ is shown versus the rescaled delay time $\gamma\tau$ for the same values of the parameters as those in Fig. 8(a). We assumed here the maximal squeezing of the field in the reservoir, i.e., $M = \sqrt{n(n+1)}$. For each of the considered cases, having the minimum of $g^{(2)}(0) < 1$, the cavity field clearly exhibits two-time PAB, $g^{(2)}(\tau) > g^{(2)}(0)$. When $\varepsilon$ takes such a value, which results in the minimal value of $g^{(2)}(0)$ for a nonmaximally squeezed reservoir field, the cavity field exhibits two-time bunching of photons for short delay time. PAB appears for longer delay time. In Figs. 2(b) and 2(c), this behavior is studied in more detail. It appears that, depending on the reservoir squeezing degree $M$ of the reservoir, both two-time photon bunching and antibunching are possible. But bunching for short delay times is possible only for such values of $M$, which result in decreasing $g^{(2)}(0)$ for increasing $M$.

### D. Nonstandard single-photon blockade of types 2 and 3

We will show now the possibility of generating nonstandard single-PB of the second and third types in the system considered here.

In Fig. 6(a), the correlation functions of $g^{(2)}(0)$, $g^{(3)}(0)$, and $g^{(4)}(0)$ are shown in their dependence on the external excitation strength $\varepsilon$ for a specified mean number of photons in the squeezed reservoir, while Fig. 6(b) shows $g^{(2)}(0)$ and $g^{(3)}(0)$ as a function of the detuning $\Delta$. As one can see, there are ranges of the excitation strengths $\varepsilon$ and the detuning $\Delta$ for which $g^{(2)}(0) < 1$ is accompanied by the additional condition for $g^{(3)}(0) > 1$, which implies the occurrence of NPB of type 2. For these regions, the condition $g^{(2)}(0) < 1$ is not sufficient for identifying "true" single-PB, because there still exists a nonzero probability of measuring more than two photons at the same time. Only the two-photon statistics is suppressed and that can be also achieved when the external driving field is off resonance with the cavity frequency. Larger values of $\varepsilon$ are related to the simultaneous suppression of the higher-order correlations. Although the values of $g^{(2)}(0)$ are increasing, still we can decrease the higher-order correlations below the value of $g^{(2)}(0)$, as shown in Fig. 6(a).

Moreover, in Fig. 4(d), we show the ranges of the squeezing $r$ and displacement $\alpha$ parameters, for which another type of nonstandard single-PB (i.e., type 3) can be observed. This NPB in Fig. 4(d) is shown in addition to the NPB of type 2 presented in Fig. 4(c).

### E. Two-photon blockade

As shown in Fig. 3, various types of single-PB can be generated via dissipation of a linearly driven optical cavity field into a squeezed environment. However, two-PB, according to the *simplified* criteria in Eq. (10), is not observed in this model, which is demonstrated in Fig. 3(e) for a specific choice of $n$. Also our numerical calculations show that it is very unlikely to generate three-PB according to the *simplified* criteria Eq. (11) for an arbitrary value of $n$.

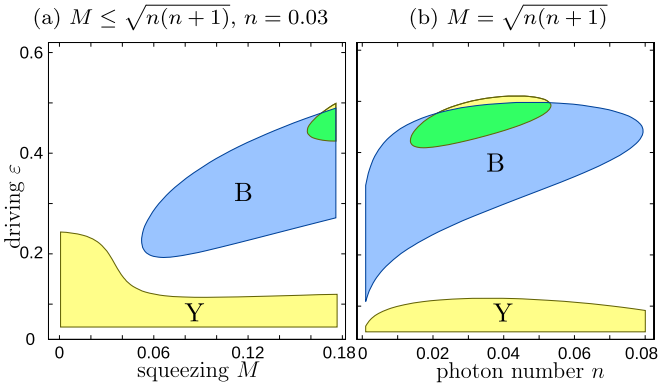


FIG. 9. Squeezed-reservoir model: two-photon blockade generated in a driven harmonic cavity coupled to a squeezed reservoir according to the refined criteria in Eq. (8) for $n = 0.03$ and (a) $M \leqslant \sqrt{n(n+1)}$ and (b) $M = \sqrt{n(n+1)}$ corresponding to the squeezed-vacuum reservoir (see Appendix B), assuming $\Delta = 0$. Specifically, by changing the driving strength $\varepsilon$ vs (a) the reservoir squeezing parameter $M$ and (b) the reservoir mean photon number $n$, we show the regions in which the criteria 1 and 2 are satisfied, as indicated in yellow and blue, respectively. Two-photon blockade occurs when both criteria 1 and 2 are satisfied, which corresponds to the green regions.

However, two-PB, according to the *refined* criteria in Eq. (8), can be observed in this model. Indeed, the green regions in Fig. 9 show the ranges of the parameters $M$, $\epsilon$, and $n$ for which two-PB can be observed.

## IV. SIMULATING VARIOUS TYPES OF PHOTON BLOCKADE AND TUNNELING WITH SQUEEZED COHERENT STATES

### A. Squeezed coherent states

Ideal SCS, or more precisely the displaced squeezed vacuum, can be obtained by applying the squeezing and displacement operators to the vacuum state as follows:

$$|\alpha, \xi\rangle = \hat{D}(\alpha)\hat{S}(\xi)|0\rangle, \tag{18}$$

where

$$\hat{S}(\xi) = \exp\left[\tfrac{1}{2}(\xi^{\star}\hat{a}^2 - \xi\hat{a}^{\dagger 2})\right] \tag{19}$$

is the squeezing operator with a complex squeezing parameter $\xi = r\exp(i\theta)$ and $D(\alpha) = \exp(\alpha\hat{a}^{\dagger} - \alpha^{\star}\hat{a})$ is the displacement operator with $\alpha = \bar{\alpha}\exp(i\phi)$, for arbitrary phases $\theta, \phi \in [0, 2\pi]$ and amplitudes $\bar{\alpha}, r \geqslant 0$.

The second-order correlation function $g^{(2)}(0)$ for the SCS with arbitrary values of $\theta$ and $\phi$ is given by

$$g^{(2)}(0) = 3 + 2(1 - 2\bar{\alpha}^2)\bar{N}^{-1} - \bar{\alpha}^2[1 + C]\bar{N}^{-2}, \tag{20}$$

where the mean photon number is

$$\bar{N} \equiv \langle\hat{a}^{\dagger}\hat{a}\rangle = \tfrac{1}{2}[2\bar{\alpha}^2 + \cosh(2r) - 1], \tag{21}$$

and $C = \cos(2\phi - \theta)\sinh(2r)$. For a special case with the optimally squeezed amplitude quadrature ($\theta = 2\phi$), Eq. (20) simplifies to the formula given in Ref. [75]. Note that such phase optimization corresponds to the so-called principal squeezing [76,83,84].

Our main objective is to determine whether two-PB (2PB) and three-PB (3PB), as well as various types of nonstandard single-PB (NPB) and other phenomena such as PIT, can be generated or simulated with squeezed states. Thus, we have to examine higher-order correlation functions, namely, $g^{(3)}(0)$ and $g^{(4)}(0)$. We find that the third-order correlation function for the SCS with arbitrary angles $\theta$ and $\phi$ is

$$g^{(3)}(0) = 15 + 9(1 - 3\bar{\alpha}^2)\bar{N}^{-1} - 9\bar{\alpha}^2(1 + B)\bar{N}^{-2} + 2\bar{\alpha}^2(2\bar{\alpha}^2 + 3C)\bar{N}^{-3}, \tag{22}$$

which considerably simplifies for the optimally squeezed amplitude quadratures ($\theta = 2\phi$).

The analytical solution of the simplified criteria in Eq. (10) can be obtained for the optimally squeezed state holding the relation of $\theta = 2\phi$. Additionally, analytical solutions can also be found whenever one of the phases is fixed and the other takes any value from the range $[0, 2\pi]$. Our numerical and analytical results show that it is very unlikely to obtain the simplified conditions in Eq. (10) for two- and three-PB for the SCS having the optimally squeezed amplitude quadratures. The same conclusion holds for the SCS with one of the phases fixed and for any values of the other phase, $\alpha$, and $r$. This conclusion has been confirmed numerically for $10^6$ randomly generated SCS without fixing any parameters.

Thus, we have shown that multi-PB, according to the simplified criteria in Eq. (10), are very unlikely for any choice of the parameters of the SCS. This suggests that, by having a physical system evolving into a squeezed state, one can expect the possibility of generating single-PB but standard squeezing does *not* lead to the generation of this type of multi-PB.

In contrast to this, we find that two-PB is still possible, but according to the refined criteria in Eq. (8). Indeed, for properly chosen parameters $M$ and $\varepsilon$ of the SCS, two-PB can be observed as shown by the green regions in Fig. 9.

Nonstandard single-PB (of type 2) can occur for the SCS. Indeed, we have found analytical solutions satisfying both criteria in Eq. (13). Such solutions exist only for some relations between the phases of the displacement and squeezing operators. The ranges of these phases are collected in Table III. The nonstandard PB effect cannot be observed for other phase relations.

### B. Displaced squeezed thermal states

In addition to the SCS, we also analyze the displaced squeezed thermal states (DSTS), which can be obtained by applying the displacement $\hat{D}(\alpha)$ and squeezing $\hat{S}(\xi)$ operators to a thermal state $\hat{\rho}_{\rm th}(n_{\rm th})$, i.e.,

$$\hat{\rho}(\alpha, \xi, n_{\rm th}) = \hat{D}(\alpha)\hat{S}(\xi)\hat{\rho}_{\rm th}(n_{\rm th})\hat{S}^{\dagger}(\xi)\hat{D}^{\dagger}(\alpha). \tag{23}$$

The thermal state is characterized by the density matrix $\hat{\rho}_{\rm th}(n_{\rm th}) = \sum_n P_n|n\rangle\langle n|$, where $P_n = n_{\rm th}^n/(1 + n_{\rm th})^{n+1}$ is the probability of finding $n$ thermal photons in a thermally excited mode having a geometric probability distribution, and $n_{\rm th}$ is the mean number of thermal photons.

TABLE III. Squeezed coherent states simulating nonstandard photon blockade (of type 2), for which $g^{(2)}(0) < 1$ and $g^{(3)}(0) > 1$ hold, vs the phase $\phi = \arg\alpha$ of the displacement operator and the phase $\theta = \arg\xi$ of the squeezing parameter.

| $\theta$ | $\phi$ | NPB |
|---|---|---|
| 0 | $(-\pi/4; \pi/4)$ and $(3\pi/4; 5\pi/4)$ | Yes |
| | $[\pi/4; 3\pi/4]$ and $[5\pi/4; 7\pi/4]$ | No |
| $\pi$ | $(\pi/4; 3\pi/4)$ and $(5\pi/4; 7\pi/4)$ | Yes |
| | $[-\pi/4; \pi/4]$ and $[3\pi/4; 5\pi/4]$ | No |
| $(-\pi/2; \pi/2)$ | $0, \pi$ | Yes |
| $[\pi/2; 3\pi/2]$ | | No |
| $[-\pi/2; \pi/2]$ | $\pi/2$ | No |
| $(\pi/2; 3\pi/2)$ | | Yes |

In Appendix E we show explicitly that the DSTS $\hat{\rho}(\alpha, \xi, n_{\rm th})$ are nonclassical if and only if the squeezing parameter $r \equiv |\xi|$ is greater than the critical value $r_0$:

$$r > r_0 \equiv \tfrac{1}{2}\ln(1 + 2n_{\rm th}). \tag{24}$$

These states are nonclassical, independent of the displacement parameter $\alpha$, because they are described by a non-positive-semidefinite Glauber-Sudarshan $P$ function. This is demonstrated in Appendix E without recalling the explicit form of the $P$ function for the DSTS. Further discussion of the nonclassical ($r > r_0$) and classical ($r \leqslant r_0$) regimes of the DSTS in relation to their simulation of PIT is presented in Sec. V.

Applying the definition of the $k$th-order correlation functions $g^{(k)}(0)$, we can easily obtain the following relations describing the second- and third-order equal-time correlation functions:

$$g^{(2)}(0) = 3 + (1 - 2\bar{\alpha}^2)\bar{N}^{-1} - h^{-}, \tag{25}$$

$$g^{(3)}(0) = 15 + 9(1 - 3\bar{\alpha}^2)\bar{N}^{-1} - 9h^{+} + 2\bar{\alpha}^2[2\bar{\alpha}^2 + 3(2n_{\rm th} + 1)B]\bar{N}^{-3}, \tag{26}$$

where the mean photon number is

$$\bar{N} \equiv \langle\hat{a}^{\dagger}\hat{a}\rangle = \tfrac{1}{2}[2\bar{\alpha}^2 + (1 + 2n_{\rm th})\cosh(2r) - 1], \tag{27}$$

and the auxiliary functions are

$$h^{\pm} = \{n_{\rm th}(1 + n_{\rm th}) + \bar{\alpha}^2[1 \pm (2n_{\rm th} + 1)C]\}\bar{N}^{-2}, \tag{28}$$

where $C$ is defined below Eq. (21). For $\theta = 2\phi$, Eqs. (25) and (26) considerably simplify. In this special case, Eq. (25) reduces to the corresponding formula given in Ref. [75].

### C. Photon correlations in squeezed coherent states

Here we analyze different kinds of PB and PIT effects as listed in Table II and shown in Figs. 3–12.

(i) Three-PT occurs when $1 < g^{(2)}(0) < g^{(3)}(0)$. We find that these conditions are satisfied for the SCS if $r > 0$ and $\alpha$ is smaller than a critical parameter $\alpha_0$, i.e.,

$$0 < \alpha < \alpha_0 \equiv \frac{1}{\sqrt{2}}\sqrt{1 + c^4 + c(2c + s)(cs - 1)}, \tag{29}$$

where hereafter $c = \cosh(r)$ and $s = \sinh(r)$.

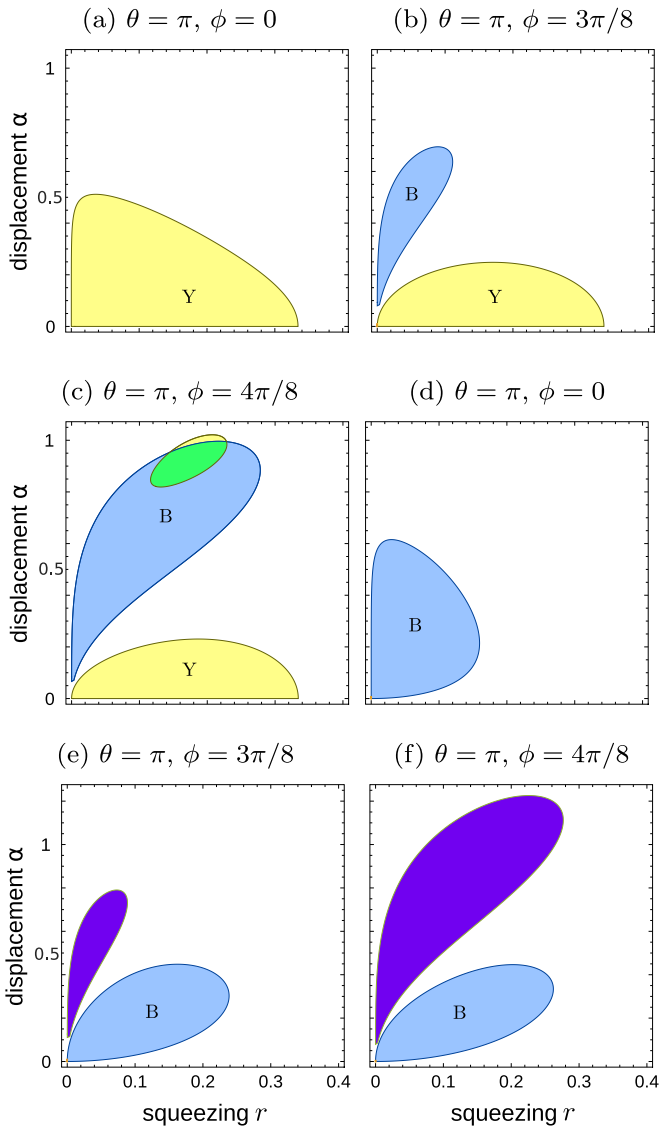


FIG. 10. Squeezed coherent states: regions of the displacement ($\alpha$) and squeezing ($r$) parameters for which the *refined* photon blockade criteria in Eq. (8) are satisfied for two-photon (a)–(c) and three-photon (d)–(f) blockades. Specifically, the regions of the SCS parameters, where the criteria 1 and 2, are satisfied for $g^{(2)}(0)$, $g^{(3)}(0)$, and $g^{(4)}(0)$, are shown in yellow, blue, and violet (or navy blue), respectively. In grayscale, yellow (indicated by "Y") is the brightest, and violet is the darkest color. Blue is marked by "B." Two-photon blockade occurs if the criteria for $g^{(2)}(0)$ and $g^{(3)}(0)$ are both satisfied, which corresponds to the green region in (c). Three-photon blockade does not occur as the regions for $g^{(3)}(0)$ and $g^{(4)}(0)$ do not overlap.

(ii) Nonstandard single-PB of type 2, which is also referred to as unconventional PB in Ref. [77], occurs if $g^{(2)}(0) < 1 < g^{(3)}(0)$, which can be observed for the SCS if $\alpha \in (\alpha_0, \alpha_1)$ for $r > 0$, where the critical parameter $\alpha_0$ is defined in Eq. (29) and another critical value of $\alpha$ is

$$\alpha_1 = \frac{1}{4\sqrt{6}s}\sqrt{3f_7 - 4(3c - 21s) + 8\sqrt{3\beta_1}(c+s)s^2}, \quad (30)$$

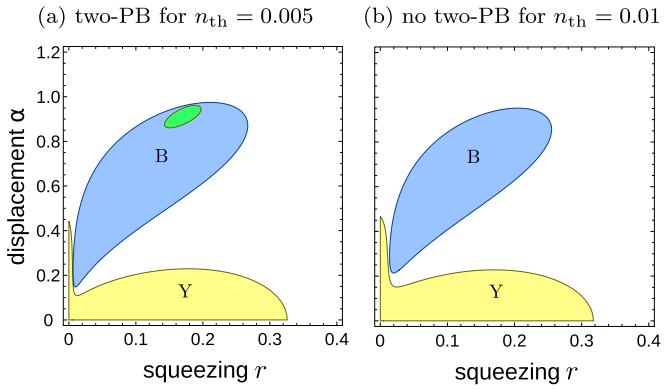


FIG. 11. Simulation of two-photon blockade with the displaced squeezed thermal states according to the refined criteria 1 and 2. Same as in Fig. 10 but for the DSTS with (a) $n_{\rm th} = 0.005$ and (b) $n_{\rm th} = 0.01$. We set here $\theta \equiv \arg\xi = \pi$ and $\phi \equiv \arg\alpha = 4\pi/8$. Two-photon blockade occurs only in panel (a) (in the green region). This green region is much larger for $n_{\rm th} = 0$ as shown in Fig. 10(c). It is seen that even a very small number of thermal photons severely shrinks the range of the parameters allowing for the observation of two-photon blockade.

given in terms of the auxiliary functions:

$$f_x = x\exp(-3r) - 4\exp(3r) + \exp(5r),$$
$$\beta_1 = 35 + 94c^4 + 2cs(70 + 47cs) - 2c^2(51 + 88cs). \quad (31)$$

(iii) Nonstandard three-PT occurs when $g^{(2)}(0) < g^{(3)}(0) < 1$. This effect can be observed for the SCS if $\alpha \in (\alpha_1, \alpha_2)$ for $r > 0$, where $\alpha_1$ is defined in Eq. (30) and

$$\alpha_2 = \frac{1}{4\sqrt{2r}}\sqrt{f_9 - 2(3c - 17s) + 8\sqrt{2\beta_2}(c+s)s^2},$$
$$\beta_2 = 10 + 29c^4 + cs(40 + 29cs) - c^2(31 + 56cs). \quad (32)$$

(iv) Single-PB is usually verified by the simplified condition $g^{(2)}(0) < 1$. Stricter conditions for single-PB can be given as $g^{(3)}(0) < g^{(2)}(0) < 1$. These conditions are satisfied for the SCS if $\alpha > \alpha_2$ and $r > 0$.

(v) Our numerical and analytical calculations show that there are no solutions for $\alpha$ satisfying the conditions $1 < g^{(3)}(0) < g^{(2)}(0)$ for two-PT.

(vi) Two-PB can indeed be observed according to the refined conditions given in Eq. (8) for both SCS and DSTS, as shown by the green regions in Figs. 10(c) and 11(a), respectively, for specific choices of the squeezing phase $\theta = \pi$ and the displacement phase $\phi = 4\pi/8$. It is seen in Figs. 10(a) and 10(b) that two-PB cannot be observed for the phases $\phi = 0, 3\pi/8$. Figures 10(c) and 11 show the destructive role of thermal photons $n_{\rm th}$ for the generation of two-PB. Indeed, the green region in Figs. 10(c) and 11 decreases with increasing $n_{\rm th}$, and it is not seen any more for $n_{\rm th} = 0.01$ in Fig. 11(b).

In contrast to this refined two-PB, our analytical and numerical calculations show that the simplified criteria in Eq. (10) for two-PB are very unlikely to be satisfied as graphically explained in Fig. 4(e) for the SCS and Fig. 5(e) for the DSTS.

Moreover, our both numerical and analytical results show that three-PB can be simulated by neither SCS nor DSTS

according to the refined and simplified criteria of PB, given in Eqs. (8) and (9), respectively. Indeed, the criteria 1 and 2 can be satisfied separately, as shown by the violet and blue regions in Figs. 10(d) and 10(e), but they cannot be satisfied simultaneously for the same values of the squeezing parameter $r$ and the displacement parameter $\alpha$. This result implies that the colored regions in these figures do not overlap.

## V. NONCLASSICAL AND CLASSICAL EFFECTS AND STATES

Now we address the question whether the analyzed effects and states are nonclassical or not.

We apply here the standard quantum-optical definition (or criterion) of the nonclassicality of a single-mode bosonic state $\hat{\rho}$ in terms of the Glauber-Sudarshan $P$ function [85]:

$$\hat{\rho} = \int d^2\beta \, P(\beta, \beta^*)|\beta\rangle\langle\beta|, \tag{33}$$

where $|\beta\rangle$ is a coherent state with a complex amplitude $\beta$. According to this common definition (see, e.g., Refs. [76,85]), a given state $\hat{\rho}$ is referred to as classical, if it is described by a classical-like (i.e., non-negative) $P$ function. Otherwise, a state $\hat{\rho}$ is considered nonclassical (or quantum), i.e., when it is described by a negative (or more precisely nonpositive or non-positive-semidefinite) $P$ function. Thus, according to this definition, *only* coherent states and their mixtures (including thermal states) can be considered classical, while all other mixed and pure states (including squeezed states) are nonclassical.

Single- and multi-PB effects are indeed purely nonclassical as shown explicitly in Appendix C.

PIT is usually also considered a quantum effect (as emphasized in, e.g., Refs. [38,60]), even if it is characterized by a classical-like property of the photon-number distributions, i.e., the second-order or higher-order super-Poissonian photon-number statistics (i.e., single-time photon bunching). We note that $g^{(2)}(0) \geqslant 1$ is usually regarded as "a general property of all kinds of classical light" [86]. Indeed, thermal states, which are classical as given by the mixtures of coherent states, can simulate PIT as shown in Appendix D.

A number of nonclassicality measures of bosonic fields have been proposed, which include nonclassical depth [87], nonclassical distance [88], and the nonclassicality volume [89], which corresponds to the volume of the negative part of the Wigner function (see, e.g., Ref. [90] and references therein). Here, we apply an entanglement potential (EP) introduced by Asbóth *et al.* [91]. Entanglement potentials are, in general, numerically and experimentally simpler than other formally defined nonclassicality measures, including the nonclassical depth and distance. Moreover, entanglement potentials are much more sensitive in detecting nonclassicality compared to the nonclassicality volume. Indeed, the nonclassicality volume of the SCS studied here is exactly zero, although the states are nonclassical according to entanglement potentials.

The basic idea of entanglement potentials is physically quite simple: By combining a classical single-mode light with the vacuum on a beam splitter (BS), then the output state is separable. In contrast to this, if the input light is nonclassical then the output light from a lossless beam splitter is entangled. Moreover, the degree of nonclassicality is not changed by lossless linear-optical transformations (including beam splitters). Thus, the degree of nonclassicality of the input state can be measured by the output-state entanglement by applying standard entanglement measures [92], e.g., the negativity, the concurrence, or the relative entropy of entanglement [91,93].

To be more specific, the nonclassicality of a single-mode state $\hat{\rho} \equiv \hat{\rho}_{\rm in}$ can be quantified, according to Ref. [91], by the entanglement of the output state $\rho_{\rm out}$ of an auxiliary lossless balanced BS with the state $\hat{\rho}$ and the vacuum $|0\rangle$ at the inputs, i.e.,

$$\hat{\rho}_{\rm out} = \hat{U}_{\rm BS}(\hat{\rho}_{\rm in} \otimes |0\rangle\langle 0|)\hat{U}_{\rm BS}^{\dagger}, \tag{34}$$

where $\hat{U}_{\rm BS}$ is the unitary transformation of a balanced (50:50) lossless beam splitter,

$$\hat{U}_{\rm BS} = \exp\left[-i\frac{\pi}{2}(\hat{a}_1^{\dagger}\hat{a}_2 + \hat{a}_1\hat{a}_2^{\dagger})\right], \tag{35}$$

and $\hat{a}_{1,2}$ ($\hat{a}_{1,2}^{\dagger}$) are the annihilation (creation) operators of the input modes. We apply here the EP based on the negativity ($N$) [91,92]:

$$\begin{aligned} {\rm EP}(\hat{\rho}_{\rm in}) &\equiv E_N(\hat{\rho}_{\rm out}) = \log_2[N(\hat{\rho}_{\rm out}) + 1] \\ &= \log_2 \left|\left|\hat{\rho}_{\rm out}^{\Gamma}\right|\right|_1, \end{aligned} \tag{36}$$

which is given in terms of the trace norm $||\hat{\rho}^{\Gamma}||_1$ of the partially transposed statistical operator $\hat{\rho}^{\Gamma}$, and the logarithmic negativity $E_N$. We note that the negativity and, thus, the corresponding entanglement potential determine, e.g., (i) the entanglement cost $E_{\rm cost} \equiv E_N$ under operations preserving the positivity of the partial transpose (at least for single-PB entangled states) [92] and (ii) the dimensionality of entanglement, which is the number of the degrees of freedom of entangled beams [35,94].

The entanglement potential, defined in Eq. (36), for the DSTS is given by the following simple formula [91]:

$${\rm EP}[\hat{\rho}(\alpha, \xi, n_{\rm th})] = \frac{r - r_0}{\ln 2}, \tag{37}$$

where the critical parameter $r_0$ is given in Eq. (24). This entanglement potential is plotted in Fig. 12(a) together with the squeezing variance, which is another nonclassicality measure of the DSTS. Indeed, in Fig. 12(b), we plotted the truncated squeezing variance defined as [95]

$$\tilde{V} \equiv \min[0, -\langle : (\Delta\hat{X}_{\varphi_0})^2 : \rangle], \tag{38}$$

where the squeezing variance for the DSTS is (see Appendix E)

$$\langle(\Delta\hat{X}_{\varphi_0})^2\rangle = \tfrac{1}{2}\left(\tfrac{1}{2} + n_{\rm th}\right)\exp(-2r) = \tfrac{1}{4}\exp[-2(r - r_0)], \tag{39}$$

and $\langle : (\Delta\hat{X}_{\varphi_0})^2 : \rangle = \langle(\Delta\hat{X}_{\varphi_0})^2\rangle - 1/4$. We note that, in general, squeezing for an optimal phase $\varphi_0$ is referred to as principal squeezing [76,83] and its geometrical interpretation can be provided by Booth's elliptical lemniscates [84]. Figure 12(b) clearly shows the same nonclassical and classical regimes of the DSTS, as those in Fig. 12(a) for the entanglement potential, as explained in greater detail in Appendix E.

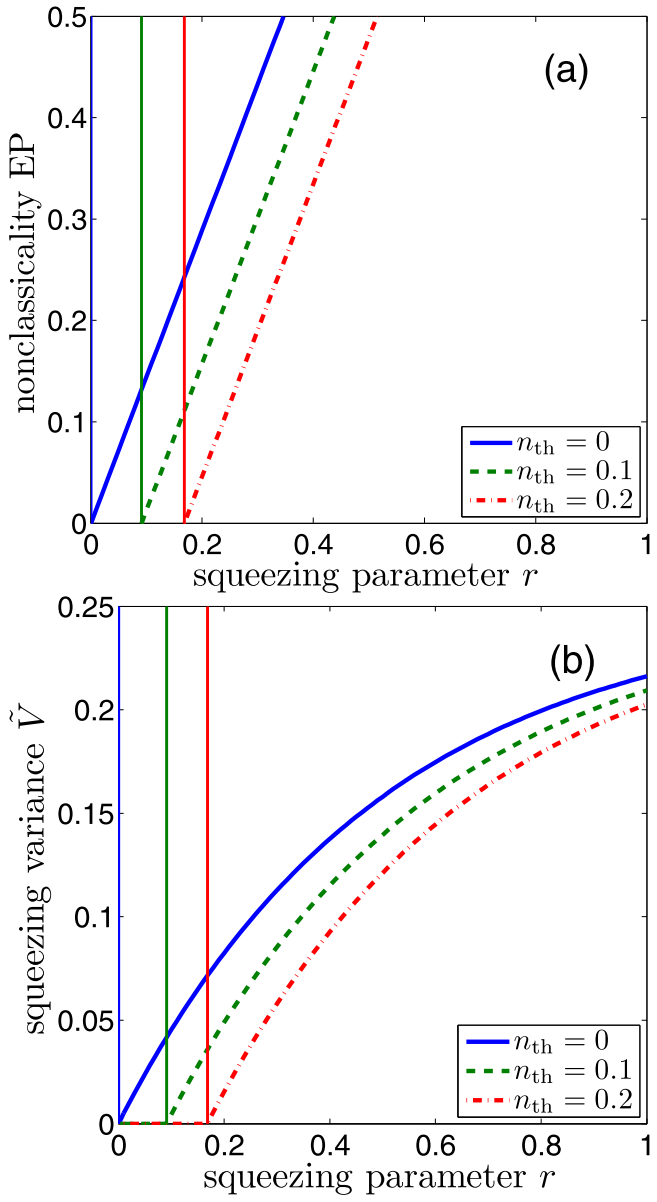


FIG. 12. Nonclassicality measures of the displaced squeezed thermal states: (a) entanglement potential, EP, of $\hat{\rho}(\alpha, \xi, n_{\rm th})$ and (b) the truncated squeezing variance $\tilde{V}$, defined in Eq. (38), vs the squeezing parameter $r = |\xi|$ for different values of the mean numbers of thermal photons $n_{\rm th}$. The EP and squeezing variance are independent of the displacement parameter $\alpha$ and the squeezing phase $\theta$. It is seen that the critical values $r_0$ (specifically, $r_0 = 0, 0.0912, 0.1682$) of the squeezing parameter $r$ increase with increasing $n_{\rm th}$ (i.e., $n_{\rm th} = 0, 0.1, 0.2$), according to Eq. (24) as indicated by the vertical thin solid lines.

By comparing Eqs. (37) and (39), it is seen that the EP is a monotonic function of the squeezing variance for the DSTS, i.e.,

$$\mathrm{EP} = -\tfrac{1}{2} \log_2 \langle (\Delta \hat{X}_{\varphi_0})^2 \rangle - 1. \tag{40}$$

Note that these quantities are also monotonically related to the nonclassical depth for the DSTS [87].

The nonclassicality of an arbitrary two-mode Gaussian state $\hat{\rho}_{\rm out}$ (which includes an arbitrary single-mode state $\hat{\rho}_{\rm in}$ studied in this paper) can also be analyzed by applying a numerically efficient nonclassicality invariant proposed in Ref. [96]. That quantifier is invariant under any global unitary photon-number-preserving transformations of the covariance matrix of a Gaussian state.

Thus, we have shown that not all our numerical predictions of PIT and other photon-number correlations correspond to quantum states, but only those for $r > r_0$ are nonclassical for the DSTS. To make this distinction clearer, we plotted in Figs. 5 and 12 the borderline at $r = r_0$ between the classical and nonclassical regimes of the DSTS. We emphasize that all SCS with nonzero squeezing parameter $r$ are nonclassical, which is a special case of the DSTS for $n_{\rm th} = 0$. Thus, all our numerical predictions shown in Figs. 4 and 10 correspond to nonclassical states.

## VI. CONCLUSIONS

Single- and two-photon blockades have been usually studied in a driven nonlinear cavity [see Fig. 1(b)] or cavities [see Fig. 1(c)] coupled to a harmonic reservoir (a thermal bath). Only a few works (including Refs. [74,75]) were devoted to the analysis of single-photon blockade via quantum nonlinear reservoir engineering.

In this paper we showed that a driven harmonic cavity coupled to a squeezed reservoir, as schematically shown in Fig. 1(a), can generate light exhibiting various types of photon blockade and related phenomena. These include two-photon blockade (as defined in Sec. II A), three-photon tunneling (defined in Sec. I D), and three nonstandard types of single-photon blockade (defined in Sec. II C), in addition to standard single-photon blockade. Our theoretical interest in studying two-photon blockade [53] has been stimulated by a recent experiment of the Rempe group [44].

As shown in Refs. [97,98], the roles of the Kerr nonlinear interaction and two-photon dissipation can be interchanged in the steady states of the systems undergoing these processes. This might explain why the linear system shown in Fig. 1(a), being coupled to a squeezed reservoir, enables the generation of photon blockade analogously to the standard Kerr nonlinear systems shown in Figs. 1(b) and 1(c) in the dispersive limit. Indeed, a squeezed reservoir allows for two-photon dissipation.

We considered various types of nonstandard photon-number-correlation effects by analyzing different properties of second- and third-order single-time correlation functions (as listed in Table II), and two-time correlations described by $g^{(2)}(\tau)$.

We also simulated these multiphoton effects with squeezed coherent states and displaced squeezed thermal states, inspired by the prediction [75] of single-photon blockade in a linear system with nonlinear damping. The relation between the squeezed-state simulations of these effects and their generation via squeezed reservoir is explained in Appendix B.

Photon blockade in nonlinear systems coupled to thermal reservoirs has already attracted considerable interest, as confirmed by a number of experimental demonstrations [37–46]. Thus, we hope that the described method of quantum reservoir engineering, which enables the generation of multiphoton blockade, photon-induced tunneling, and related phenomena,

can also stimulate further theoretical and experimental research in optical and microwave photonics [17].


## ACKNOWLEDGMENTS

The authors kindly acknowledge insightful discussions with Fabrizio Minganti and Wei Qin. J.P. is supported by GA ČR Project No. 18-22102S. F.N. is supported in part by the Multidisciplinary University Research Initiative Center for Dynamic Magneto-Optics via the Air Force Office of Scientific Research (Grant No. FA9550-14-1-0040), Asian Office of Aerospace Research and Development (Grant No. FA2386-18-1-4045), Japan Science and Technology Agency (via the Q-LEAP program and CREST Grant No. JPMJCR1676), Japan Society for the Promotion of Science (JSPS) (JSPS-RFBR Grant No. 17-52-50023 and JSPS-FWO Grant No. VS.059.18N), the FQXi, the NTT PHi Lab, and the RIKEN-AIST Challenge Research Fund. Finally, F.N. and A.M. are supported by the Army Research Office (Grant No. W911NF-18-1-0358).


## APPENDIX A: STANDARD SYSTEMS FOR STUDYING CONVENTIONAL AND UNCONVENTIONAL PHOTON BLOCKADE

For a better comparison of the proposed PB system shown in Fig. 1(a), we briefly recall here the prototype systems for generating conventional [see Fig. 1(b)] and unconventional [see Fig. 1(c)] PB effects.

(1) Conventional PB is usually studied in a driven Kerr nonlinear system described by the Hamiltonian

$$\hat{H}_a = \omega_c \hat{a}^\dagger \hat{a} + \varepsilon(\hat{a}e^{i\omega_d t} + \hat{a}^\dagger e^{-i\omega_d t}) + \chi \hat{a}^\dagger \hat{a}^\dagger \hat{a}\hat{a}, \tag{A1}$$

where $\chi$ is a Kerr nonlinearity proportional to the third-order susceptibility $\chi^{(3)}$, and the other terms of this Hamiltonian are the same as in Eq. (15). The Hamiltonian (A1) can be effectively derived (see, e.g., Ref. [53] and references therein) from the Jaynes-Cummings model in the dispersive limit (i.e., far off resonance) describing a driven cavity interacting with a two-level system (qubit) under the rotating wave approximation. Thus, the system shown schematically in Fig. 1(b) can be given by the Hamiltonian

$$\begin{aligned}\hat{H}_a^q = {} & \tfrac{1}{2}\omega\hat{\sigma}_z + \omega_c \hat{a}^\dagger \hat{a} + g(\hat{\sigma}^+ \hat{a} + \hat{a}^\dagger \hat{\sigma}^-) \\ & + \varepsilon(\hat{a}e^{i\omega_d t} + \hat{a}^\dagger e^{-i\omega_d t}),\end{aligned} \tag{A2}$$

where $\hat{\sigma}^-$ ($\hat{\sigma}^+$) is the qubit lowering (raising) operator; $\sigma_z = |e\rangle\langle e| - |g\rangle\langle g|$ is a Pauli operator; and $|g\rangle$ ($|e\rangle$) is the ground (excited) state of the two-level system.

(2) The prototype Hamiltonian for generating unconventional PB is given by [47–50]

$$\hat{H}_{ab} = \hat{H}_a + \hat{H}_b + J\hat{a}^\dagger \hat{b} + J^* \hat{a}\hat{b}^\dagger, \tag{A3}$$

where

$$\hat{H}_b = \omega_c' \hat{b}^\dagger \hat{b} + \varepsilon'(\hat{b}e^{i\omega_d' t} + \hat{b}^\dagger e^{-i\omega_d' t}) + \chi' \hat{b}^\dagger \hat{b}^\dagger \hat{b}\hat{b}, \tag{A4}$$

where $\hat{b}$ ($\hat{b}^\dagger$) is the annihilation (creation) operator of the optical mode in the second cavity, $\chi'$ is the Kerr nonlinearity of the second cavity, and the quantities $\omega_c'$, $\omega_d'$, and $\varepsilon'$ correspond, respectively, to $\omega_c$, $\omega_d$, and $\varepsilon$ in Eq. (15), but for the second cavity.

In analogy to the derivation of the conventional Kerr-nonlinear Hamiltonian in Eq. (A1) from Eq. (A2), also Eq. (A3) can be derived from the two linearly coupled driven Jaynes-Cummings systems in the dispersive limit. Such a two-cavity system can be described by

$$\hat{H}_{ab}^q = \hat{H}_a^q + \hat{H}_b^q + J\hat{a}^\dagger \hat{b} + J^* \hat{a}\hat{b}^\dagger, \tag{A5}$$

where $\hat{H}_b^q$ is defined analogously to $\hat{H}_a^q$ in Eq. (A2), but for the mode $\hat{b}$ of the second cavity. This two-atom system can be simplified to include only one atom, which is the case shown in Fig. 1(c).

The dissipative evolution of such PB systems has been usually studied assuming their coupling to a thermal reservoir within the Lindblad master equation,

$$\frac{d\hat{\rho}}{dt} = -i[\hat{H}, \hat{\rho}] + \frac{1}{2}\gamma\{(n_{\rm th}+1)\Gamma_1[\hat{a}]\hat{\rho} + n_{\rm th}\Gamma_1[\hat{a}^\dagger]\hat{\rho}\}, \tag{A6}$$

for the reduced density matrix $\hat{\rho}$, where the Lindblad superoperator $\Gamma_1[\hat{x}]\hat{\rho}$ is defined in Eq. (B2) in Appendix B, $\gamma$ is the damping rate, and $n_{\rm th} = \{\exp[\hbar\omega/(k_B T)] - 1\}^{-1}$ is the mean thermal photon number.

## APPENDIX B: MASTER EQUATION FOR THE SQUEEZED-VACUUM RESERVOIR

Here, we show more explicitly the relation between squeezed states and a squeezed reservoir by studying the master equation for the squeezed-vacuum reservoir, given in Eq. (17) in its special case for $|M| = \sqrt{n(n+1)}$. Our presentation is based on Refs. [80–82] (see also, e.g., Ref. [99]).

The master equation in Eq. (17), with the system Hamiltonian $\hat{H}$ in Eq. (16), can be rewritten more compactly as

$$\begin{aligned}\frac{d\hat{\rho}}{dt} = {} & -i[\hat{H}, \hat{\rho}] + \frac{1}{2}\gamma\{(n+1)\Gamma_1[\hat{a}]\hat{\rho} + n\Gamma_1[\hat{a}^\dagger]\hat{\rho} \\ & - M\Gamma_2[\hat{a}]\hat{\rho} - M^*\Gamma_2[\hat{a}^\dagger]\hat{\rho}\},\end{aligned} \tag{B1}$$

using the superoperators defined as

$$\Gamma_1[\hat{x}]\hat{\rho} = 2\hat{x}\hat{\rho}\hat{x}^\dagger - \hat{x}^\dagger\hat{x}\hat{\rho} - \hat{\rho}\hat{x}^\dagger\hat{x}, \tag{B2}$$

$$\Gamma_2[\hat{x}]\hat{\rho} = 2\hat{x}\hat{\rho}\hat{x} - \hat{x}\hat{x}\hat{\rho} - \hat{\rho}\hat{x}\hat{x}. \tag{B3}$$

This master equation can be derived by considering a system described by $\hat{H}'$ in Eq. (15) or, equivalently, $\hat{H}$ in Eq. (16), with its cavity mode $\hat{a}$ being linearly coupled to an infinite set of reservoir modes $\hat{b}_k$ [99]. We assume that the reservoir modes $\hat{b}_k$ are initially in the squeezed vacuum states,

$$|\vec{\xi}\,\rangle = \prod_k |\xi_k\rangle = \prod_k \hat{S}_k(\xi)|0_k\rangle, \tag{B4}$$

where the $k$th-mode squeezing operator is given by

$$\hat{S}_k = \exp\left(\xi^* \hat{b}_{k_0+k}\hat{b}_{k_0-k} - \text{H.c.}\right), \tag{B5}$$

where $k_0 = \omega_c/c$, $\xi = r\exp(i\theta)$ is the usual complex squeezing parameter, and H.c. denotes the corresponding Hermitian-conjugate term. Thus, $\hat{S}_k$ in Eq. (B5) is a two-mode squeezing operator for each $k$. Note that the master equation in Eq. (B1) can also be derived for a single-mode squeezing operator acting on each reservoir mode $k$ [81]. The total initial state

is assumed to be $\hat{\rho}_T = \hat{\rho}(0) \otimes |\vec{\xi}\,\rangle\langle\vec{\xi}\,|$, and the total system-reservoir Hamiltonian reads

$$\hat{H}_T = \hat{H}' + \sum_k \omega_k \hat{b}_k^\dagger \hat{b}_k + \sum_k g_k(\hat{a}\hat{b}_k^\dagger + \hat{a}^\dagger b_k), \tag{B6}$$

where $g_k$ is the coupling strength between the system mode $\hat{a}$ and the reservoir mode $\hat{b}_k$. The standard procedure of deriving the equation of motion for the reduced density matrix $\hat{\rho}$ under the Markov approximation results in the master equation, given in Eq. (B1) in the interaction picture, where

$$\begin{aligned} \langle \hat{b}_k^\dagger \hat{b}_{k'} \rangle &= n\delta_{kk'} = \sinh^2(r)\delta_{kk'}, \\ \langle \hat{b}_k \hat{b}_{k'} \rangle &= -M^*\delta_{k'k''} = -\cosh(r)\sinh(r)e^{i\theta}\delta_{k'k''}, \end{aligned} \tag{B7}$$

with $k'' = 2k_0 - k$. By applying the Bogoliubov transformation,

$$\begin{aligned} \hat{a}_s &= \hat{S}^\dagger \hat{a} \hat{S} = \cosh(r)\hat{a} - \sinh(r)e^{i\theta}\hat{a}^\dagger, \\ \hat{a}_s^\dagger &= \hat{S}^\dagger \hat{a}^\dagger \hat{S} = \cosh(r)\hat{a}^\dagger - \sinh(r)e^{-i\theta}\hat{a}, \end{aligned} \tag{B8}$$

where $\hat{S}(\xi)$ is the squeezing operator defined in Eq. (19), the master equation in Eq. (B1) for $\Delta = 0$ reduces, in the squeezed-vacuum frame, to the standard-form master equation without $\Gamma_2$ terms, i.e.,

$$\frac{d\hat{\rho}}{dt} = -i[\hat{H}_s, \hat{\rho}] + \frac{\gamma}{2}\Gamma_1[\hat{a}_s]\hat{\rho}, \tag{B9}$$

or, equivalently,

$$\frac{d\hat{\rho}_s}{dt} = -i[\hat{H}, \hat{\rho}_s] + \frac{\gamma}{2}\Gamma_1[\hat{a}]\hat{\rho}_s, \tag{B10}$$

where $\hat{\rho}_s = \hat{S}\rho\hat{S}^\dagger$ and

$$\hat{H}_s = \hat{S}^\dagger \hat{H} \hat{S} = \varepsilon(\hat{a}_s^\dagger + \hat{a}_s). \tag{B11}$$

As mentioned above, the resonant case $\Delta = 0$ is assumed here. Note that for $\Delta \neq 0$ terms proportional to $\hat{a}^2$ and $(\hat{a}^\dagger)^2$ should be added to the master equations in (B9) and (B10).

## APPENDIX C: NONCLASSICALITY OF PHOTON BLOCKADE

Here we recall that PB is a nonclassical effect. First we show this for single-PB using the $P$-function approach. And then we apply another approach for any multi-PB.

We first recall that $(\hat{a}^\dagger)^2\hat{a}^2 = \hat{n}(\hat{n}-1) =: \hat{n}^2 :$, where :: means the normal ordering of the creation and annihilation operators. The photon-number variance $\langle : (\Delta\hat{n})^2 : \rangle$ is simply related to $g^{(2)}(0)$ as follows:

$$\langle : (\Delta\hat{n})^2 : \rangle = \langle : \hat{n}^2 : \rangle - \langle \hat{n} \rangle^2 = [g^{(2)}(0) - 1]\langle \hat{n} \rangle^2, \tag{C1}$$

where $\Delta\hat{n} = \hat{n} - \langle \hat{n} \rangle$. So, $g^{(2)}(0) < 1$ if and only if the variance is negative:

$$\langle : (\Delta\hat{n})^2 : \rangle = \int d^2\beta\, P(\beta, \beta^*)(|\beta|^2 - \langle \hat{n} \rangle)^2 < 0. \tag{C2}$$

Because the terms $(|\beta|^2 - \langle \hat{n} \rangle)^2 \geqslant 0$ and $\langle : (\Delta\hat{n})^2 : \rangle < 0$, then $P(\beta, \beta^*)$ must also be negative in some regions of phase space. This means that the state $\hat{\rho}$, which exhibits single-PB, is described by a non-positive-semidefinite $P(\beta, \beta^*)$, and, thus, has to be nonclassical.

The nonclassicality of single- and multi-PB can be shown even faster by recalling the following facts: (1) classical states of light are either coherent states or their mixtures; (2) coherent states are characterized by $g^{(k)}(0) = 1$, for any $k \geqslant 1$; (3) $k$-PB requires $g^{(k+1)}(0) < 1$, or even the sharper condition $g^{(k+1)}(0) < A \equiv \exp(-\langle \hat{n} \rangle) \leqslant 1$, according to the refined PB criterion 1 in Eq. (8). So, single- and multi-PB can occur only for photon-number distributions which are sharper [79] than that of a coherent state and, therefore, also sharper than any mixtures of coherent states. This completes our proofs.

## APPENDIX D: CLASSICAL SIMULATION OF PHOTON-INDUCED TUNNELING WITH THERMAL STATES

Here we show that usual thermal states can simulate the PIT of an arbitrary number of photons.

The thermal-state probability $P_n$ of measuring $n$ photons can be compactly written as $P_n = yx^n$, where $x = \langle \hat{n} \rangle y$, $y = 1/(1 + \langle \hat{n} \rangle)$, and $\langle \hat{n} \rangle \equiv \bar{n}_{\rm th} = \{\exp[\hbar\omega/(k_B T)] - 1\}^{-1}$. Then the geometric series for the second- and higher-order correlation functions $g^{(k)}(0)$ can be easily calculated as

$$\begin{aligned} g^{(2)}(0) &= \frac{y}{\langle \hat{n} \rangle^2} \sum_n x^n n(n-1) = 2, \\ g^{(3)}(0) &= \frac{y}{\langle \hat{n} \rangle^3} \sum_n x^n n(n-1)(n-2) = 6. \end{aligned} \tag{D1}$$

These values can also be obtained from Eqs. (25) and (26) in their special cases for $\alpha = r = 0$.

By induction, we conclude that for any order $k > 1$ the correlation function $g^{(k)}(0)$ for the thermal state with the mean photon number $\langle \hat{n} \rangle$ becomes

$$g^{(k)}(0) = \langle \hat{n} \rangle^{-k} \sum_n P_n n^{[k]} = k!, \tag{D2}$$

where $n^{[k]} = n(n-1)\cdots(n-k+1)$. This implies that for any $k > 1$ and $\langle \hat{n} \rangle > 0$ the following holds:

$$1 < g^{(k)}(0) < g^{(k+1)}(0). \tag{D3}$$

Thus, thermal states can simulate the PIT of any number of (thermal) photons. In particular, this includes two- and three-PT, which are characterized by the conditions $1 < g^{(2)}(0)$ and Eq. (3), respectively.

## APPENDIX E: NONCLASSICAL AND CLASSICAL REGIMES OF DISPLACED SQUEEZED THERMAL STATES

For completeness of our presentation, we show explicitly that the DSTS, given by $\hat{\rho}(\alpha, \xi, n_{\rm th})$, are nonclassical if the inequality $|\xi| > r_0$, given in Eq. (24), is satisfied.

By defining a phase-dependent quadrature operator

$$\hat{X}_\varphi = \tfrac{1}{2}[\hat{a}\exp(i\varphi) + \hat{a}^\dagger \exp(-i\varphi)], \tag{E1}$$

the minimum value of the normally ordered variance $\langle:(\Delta\hat{X}_\varphi)^2:\rangle$ for the DSTS is given by

$$\min_{\varphi}\langle:(\Delta\hat{X}_\varphi)^2:\rangle \equiv \langle:(\Delta\hat{X}_{\varphi_0})^2:\rangle = \tfrac{1}{4}\exp[-2(r-r_0)] - \tfrac{1}{4}, \tag{E2}$$

where $\varphi_0$ denotes the optimal value of the quadrature phase $\varphi$. In particular, $\varphi_0 = 0$ for the squeezing phase $\theta = 0$. Moreover, :: denotes normal ordering and $\Delta\hat{X}_\varphi = \hat{X}_\varphi - \langle\hat{X}_\varphi\rangle$. It is seen that Eq. (E2) is independent of the displacement parameter $\alpha$ and, thus, equivalent to the variance for the squeezed thermal states first derived in Ref. [100].

Squeezing occurs if $\langle:(\Delta X_\varphi)^2:\rangle < 0$. This normally ordered variance can be directly calculated from the corresponding $P$ function:

$$\langle:(\Delta X_{\varphi_0})^2:\rangle = \int d^2\beta\, P(\beta,\beta^*)[X_{\varphi_0}(\beta,\beta^*) - \langle\hat{X}_{\varphi_0}\rangle]^2 < 0, \tag{E3}$$

where

$$X_{\varphi_0} = \tfrac{1}{2}[\beta\exp(i\varphi_0) + \beta^*\exp(-i\varphi_0)]. \tag{E4}$$

Because the term $[...]^2$ is non-negative and $\langle:(\Delta X_{\varphi_0})^2:\rangle$ is negative for any squeezed state, then $P(\beta,\beta^*)$ has to be negative in some regions of phase space. This means that the DSTS for $r > r_0$ are nonclassical. This result is confirmed by Eq. (37) for the entanglement potential, and shown in Fig. 12. Thus, the requirement $r > r_0$ is the necessary and sufficient condition of the $P$-function-based nonclassicality for the DSTS. This implies that any nonclassical DSTS exhibits quadrature squeezing.

In a special case of the SCS, given by $|\alpha,\xi\rangle = \hat{D}(\alpha)\hat{S}(\xi)|0\rangle$, we recover the well-known result that $r_0 = 0$, which means that any SCS with a nonzero squeezing parameter is nonclassical [3].

Thus, to show the nonclassicality of the DSTS, we have plotted the entanglement potential and the squeezing variance in Figs. 12(a) and 12(b), respectively. Moreover, we plotted the red vertical line at $r = r_0$ in Fig. 5 to show more explicitly the borderline between the classical and nonclassical regimes of the DSTS.


[1] V. Dodonov, "Nonclassical" states in quantum optics: A 'squeezed' review of the first 75 years, J. Opt. B: Quant. Semiclass. Opt. **4**, R1 (2002).

[2] D. F. Walls, Squeezed states of light, Nature (London) **306**, 141 (1983).

[3] R. Loudon and P. Knight, Squeezed Light, J. Mod. Opt. **34**, 709 (1987).

[4] *Theory of Nonclassical States of Light*, edited by V. Dodonov and V. Man'ko (Taylor & Francis, London, 2002).

[5] *Quantum Squeezing*, edited by P. D. Drummond and Z. Ficek (Springer-Verlag, Berlin, 2004).

[6] U. L. Andersen, T. Gehring, C. Marquardt, and G. Leuchs, 30 years of squeezed light generation, Phys. Scr. **91**, 053001 (2016).

[7] E. H. Kennard, Zur Quantenmechanik einfacher Bewegungstypen, Z. Phys. **44**, 326 (1927).

[8] L. Infeld and J. Plebański, On a certain class of unitary transformations, Acta Phys. Pol. **14**, 41 (1955).

[9] J. Plebański, Wave functions of a harmonic oscillator, Phys. Rev. **101**, 1825 (1956).

[10] J. N. Hollenhorst, Quantum limits on resonant-mass gravitational-radiation detectors, Phys. Rev. D **19**, 1669 (1979).

[11] C. M. Caves, K. S. Thorne, R. W. P. Drever, V. D. Sandberg, and M. Zimmermann, On the measurement of a weak classical force coupled to a quantum-mechanical oscillator. I. Issues of principle, Rev. Mod. Phys. **52**, 341 (1980).

[12] V. Dodonov, V. Man'ko, and V. Rudenko, Nondemolition measurements in gravitational-wave experiments, Sov. Phys. JETP **51**, 443 (1980).

[13] C. M. Caves, Quantum-mechanical noise in an interferometer, Phys. Rev. D **23**, 1693 (1981).

[14] R. E. Slusher, L. W. Hollberg, B. Yurke, J. C. Mertz, and J. F. Valley, Observation of Squeezed States Generated by Four-Wave Mixing in an Optical Cavity, Phys. Rev. Lett. **55**, 2409 (1985).

[15] L.-A. Wu, H. J. Kimble, J. L. Hall, and H. Wu, Generation of Squeezed States by Parametric Down Conversion, Phys. Rev. Lett. **57**, 2520 (1986).

[16] R. M. Shelby, M. D. Levenson, S. H. Perlmutter, R. G. DeVoe, and D. F. Walls, Broad-Band Parametric Deamplification of Quantum Noise in an Optical Fiber, Phys. Rev. Lett. **57**, 691 (1986).

[17] X. Gu, A. F. Kockum, A. Miranowicz, Y.-X. Liu, and F. Nori, Microwave photonics with superconducting quantum circuits, Phys. Rep. **718–719**, 1 (2017).

[18] LIGO Scientific Collaboration, Enhanced sensitivity of the LIGO gravitational wave detector by using squeezed states of light, Nat. Photonics **7**, 613 (2013).

[19] H. Grote, K. Danzmann, K. L. Dooley, R. Schnabel, J. Slutsky, and H. Vahlbruch, First Long-Term Application of Squeezed States of Light in a Gravitational-Wave Observatory, Phys. Rev. Lett. **110**, 181101 (2013).

[20] M. Bartkowiak, L.-A. Wu, and A. Miranowicz, Quantum circuits for amplification of Kerr nonlinearity via quadrature squeezing, J. Phys. B **47**, 145501 (2014).

[21] X.-Y. Lü, Y. Wu, J. R. Johansson, H. Jing, J. R. Zhang, and F. Nori, Squeezed Optomechanics with Phase-Matched Amplification and Dissipation, Phys. Rev. Lett. **114**, 093602 (2015).

[22] M.-A. Lemonde, N. Didier, and A. A. Clerk, Enhanced nonlinear interactions in quantum optomechanics via mechanical amplification, Nat. Commun. **7**, 11338 (2016).

[23] W. Qin, A. Miranowicz, P.-B. Li, X.-Y. Lü, J. Q. You, and F. Nori, Exponentially Enhanced Light-Matter Interaction, Cooperativities, and Steady-State Entanglement Using Parametric Amplification, Phys. Rev. Lett. **120**, 093601 (2018).

[24] C. Leroux, L. C. G. Govia, and A. A. Clerk, Enhancing Cavity Quantum Electrodynamics via Antisqueezing: Synthetic Ultrastrong Coupling, Phys. Rev. Lett. **120**, 093602 (2018).

[25] W. Qin, V. Macri, A. Miranowicz, S. Savasta, and F. Nori, Emission of photon pairs by mechanical stimulation of the squeezed vacuum, Phys. Rev. A (to be published), arXiv:1902.04216.

[26] A. F. Kockum, A. Miranowicz, S. D. Liberato, S. Savasta, and F. Nori, Ultrastrong coupling between light and matter, Nat. Rev. Phys. **1**, 19 (2019).

[27] A. Ridolfo, M. Leib, S. Savasta, and M. J. Hartmann, Photon Blockade in the Ultrastrong Coupling Regime, Phys. Rev. Lett. **109**, 193602 (2012).

[28] A. Le Boité, M.-J. Hwang, H. Nha, and M. B. Plenio, Fate of photon blockade in the deep strong-coupling regime, Phys. Rev. A **94**, 033827 (2016).

[29] A. Imamoğlu, H. Schmidt, G. Woods, and M. Deutsch, Strongly Interacting Photons in a Nonlinear Cavity, Phys. Rev. Lett. **79**, 1467 (1997).

[30] W. Leoński and A. Kowalewska-Kudłaszyk, Quantum Scissors: Finite-Dimensional States Engineering, Prog. Opt. **56**, 131 (2011).

[31] L. Tian and H. J. Carmichael, Quantum trajectory simulations of two-state behavior in an optical cavity containing one atom, Phys. Rev. A **46**, R6801(R) (1992).

[32] W. Leoński and R. Tanaś, Possibility of producing the one-photon state in a kicked cavity with a nonlinear Kerr medium, Phys. Rev. A **49**, R20(R) (1994).

[33] Y.-X. Liu, A. Miranowicz, Y. B. Gao, J. Bajer, C. P. Sun, and F. Nori, Qubit-induced phonon blockade as a signature of quantum behavior in nanomechanical resonators, Phys. Rev. A **82**, 032101 (2010).

[34] N. Didier, S. Pugnetti, Y. M. Blanter, and R. Fazio, Detecting phonon blockade with photons, Phys. Rev. B **84**, 054503 (2011).

[35] A. Miranowicz, J. Bajer, N. Lambert, Y.-X. Liu, and F. Nori, Tunable multiphonon blockade in coupled nanomechanical resonators, Phys. Rev. A **93**, 013808 (2016).

[36] X. Wang, A. Miranowicz, H.-R. Li, and F. Nori, Method for observing robust and tunable phonon blockade in a nanomechanical resonator coupled to a charge qubit, Phys. Rev. A **93**, 063861 (2016).

[37] K. M. Birnbaum, A. Boca, R. Miller, A. D. Boozer, T. E. Northup, and H. J. Kimble, Photon blockade in an optical cavity with one trapped atom, Nature (London) **436**, 87 (2005).

[38] A. Faraon, I. Fushman, D. Englund, N. Stoltz, P. Petroff, and J. Vučković, Coherent generation of non-classical light on a chip via photon-induced tunnelling and blockade, Nat. Phys. **4**, 859 (2008).

[39] C. Lang, D. Bozyigit, C. Eichler, L. Steffen, J. M. Fink, A. A. Abdumalikov, M. Baur, S. Filipp, M. P. da Silva, A. Blais, and A. Wallraff, Observation of Resonant Photon Blockade at Microwave Frequencies Using Correlation Function Measurements, Phys. Rev. Lett. **106**, 243601 (2011).

[40] A. J. Hoffman, S. J. Srinivasan, S. Schmidt, L. Spietz, J. Aumentado, H. E. Türeci, and A. A. Houck, Dispersive Photon Blockade in a Superconducting Circuit, Phys. Rev. Lett. **107**, 053602 (2011).

[41] A. Reinhard, T. Volz, M. Winger, A. Badolato, K. J. Hennessy, E. L. Hu, and A. Imamoğlu, Strongly correlated photons on a chip, Nat. Photonics **6**, 93 (2011).

[42] T. Peyronel, O. Firstenberg, Q.-Y. Liang, S. Hofferberth, A. V. Gorshkov, T. Pohl, M. D. Lukin, and V. Vuletić, Quantum nonlinear optics with single photons enabled by strongly interacting atoms, Nature (London) **488**, 57 (2012).

[43] K. Müller, A. Rundquist, K. A. Fischer, T. Sarmiento, K. G. Lagoudakis, Y. A. Kelaita, C. Sánchez Muñoz, E. del Valle, F. P. Laussy, and J. Vučković, Coherent Generation of Nonclassical Light on Chip via Detuned Photon Blockade, Phys. Rev. Lett. **114**, 233601 (2015).

[44] C. Hamsen, K. N. Tolazzi, T. Wilk, and G. Rempe, Two-Photon Blockade in an Atom-Driven Cavity QED System, Phys. Rev. Lett. **118**, 133604 (2017).

[45] H. J. Snijders, J. A. Frey, J. Norman, H. Flayac, V. Savona, A. C. Gossard, J. E. Bowers, M. P. van Exter, D. Bouwmeester, and W. Löffler, Observation of the Unconventional Photon Blockade, Phys. Rev. Lett. **121**, 043601 (2018).

[46] C. Vaneph, A. Morvan, G. Aiello, M. Féchant, M. Aprili, J. Gabelli, and J. Estève, Observation of the Unconventional Photon Blockade in the Microwave Domain, Phys. Rev. Lett. **121**, 043602 (2018).

[47] W. Leoński and A. Miranowicz, Kerr nonlinear coupler and entanglement, J. Opt. B **6**, S37 (2004).

[48] A. Miranowicz and W. Leoński, Two-mode optical state truncation and generation of maximally entangled states in pumped nonlinear couplers, J. Phys. B **39**, 1683 (2006).

[49] T. C. H. Liew and V. Savona, Single Photons from Coupled Quantum Modes, Phys. Rev. Lett. **104**, 183601 (2010).

[50] M. Bamba, A. Imamoğlu, I. Carusotto, and C. Ciuti, Origin of strong photon antibunching in weakly nonlinear photonic molecules, Phys. Rev. A **83**, 021802(R) (2011).

[51] H. Flayac and V. Savona, Unconventional photon blockade, Phys. Rev. A **96**, 053810 (2017).

[52] S. Shamailov, A. Parkins, M. Collett, and H. Carmichael, Multi-photon blockade and dressing of the dressed states, Opt. Commun. **283**, 766 (2010).

[53] A. Miranowicz, M. Paprzycka, Y.-X. Liu, J. Bajer, and F. Nori, Two-photon and three-photon blockades in driven nonlinear systems, Phys. Rev. A **87**, 023809 (2013).

[54] G. H. Hovsepyan, A. R. Shahinyan, and G. Y. Kryuchkyan, Multiphoton blockades in pulsed regimes beyond stationary limits, Phys. Rev. A **90**, 013839 (2014).

[55] H. J. Carmichael, Breakdown of Photon Blockade: A Dissipative Quantum Phase Transition in Zero Dimensions, Phys. Rev. X **5**, 031028 (2015).

[56] W.-W. Deng, G.-X. Li, and H. Qin, Enhancement of the two-photon blockade in a strong-coupling qubit-cavity system, Phys. Rev. A **91**, 043831 (2015).

[57] C. J. Zhu, Y. P. Yang, and G. S. Agarwal, Collective multiphoton blockade in cavity quantum electrodynamics, Phys. Rev. A **95**, 063842 (2017).

[58] S. Felicetti, D. Z. Rossatto, E. Rico, E. Solano, and P. Forn-Díaz, Two-photon quantum Rabi model with superconducting circuits, Phys. Rev. A **97**, 013851 (2018).

[59] S. Felicetti, M.-J. Hwang, and A. Le Boité, Ultrastrong-coupling regime of nondipolar light-matter interactions, Phys. Rev. A **98**, 053859 (2018).

[60] R. Huang, A. Miranowicz, J.-Q. Liao, F. Nori, and H. Jing, Nonreciprocal Photon Blockade, Phys. Rev. Lett. **121**, 153601 (2018).

[61] B. Li, R. Huang, X. Xu, A. Miranowicz, and H. Jing, Nonreciprocal unconventional photon blockade in a spinning optomechanical system, Photonics Res. **7**, 630 (2019).

[62] A. Miranowicz, W. Leoński, S. Dyrting, and R. Tanaś, Quantum state engineering in finite-dimensional Hilbert space, Acta Phys. Slov. **46**, 451 (1996).

[63] W. Leoński, Fock states in a Kerr medium with parametric pumping, Phys. Rev. A **54**, 3369 (1996).

[64] W. Leoński and A. Miranowicz, Quantum-optical states in finite-dimensional Hilbert space. II. State generation, Adv. Chem. Phys. **119**, 195 (2001).

[65] W. Leoński, Finite-dimensional coherent-state generation and quantum-optical nonlinear oscillator models, Phys. Rev. A **55**, 3874 (1997).

[66] A. Miranowicz, K. Piątek, and R. Tanaś, Coherent states in a finite-dimensional Hilbert space, Phys. Rev. A **50**, 3423 (1994).

[67] A. Miranowicz, W. Leoński, and N. Imoto, Quantum-optical states in finite-dimensional Hilbert space. I. General formalism, Adv. Chem. Phys. **119**, 155 (2001).

[68] Y.-X. Liu, X.-W. Xu, A. Miranowicz, and F. Nori, From blockade to transparency: Controllable photon transmission through a circuit-QED system, Phys. Rev. A **89**, 043818 (2014).

[69] A. Majumdar, M. Bajcsy, A. Rundquist, and J. Vučković, Loss-Enabled Sub-Poissonian Light Generation in a Bimodal Nanocavity, Phys. Rev. Lett. **108**, 183601 (2012).

[70] A. Majumdar, M. Bajcsy, and J. Vučković, Probing the ladder of dressed states and nonclassical light generation in quantum-dot–cavity QED, Phys. Rev. A **85**, 041801(R) (2012).

[71] X.-W. Xu, Y.-J. Li, and Y.-X. Liu, Photon-induced tunneling in optomechanical systems, Phys. Rev. A **87**, 025803 (2013).

[72] A. Rundquist, M. Bajcsy, A. Majumdar, T. Sarmiento, K. Fischer, K. G. Lagoudakis, S. Buckley, A. Y. Piggott, and J. Vučković, Nonclassical higher-order photon correlations with a quantum dot strongly coupled to a photonic-crystal nanocavity, Phys. Rev. A **90**, 023846 (2014).

[73] C. Zhai, R. Huang, H. Jing, and L.-M. Kuang, Mechanical switch of photon blockade and photon-induced tunneling, Opt. Express **27**, 27649 (2019).

[74] A. Miranowicz, J. Bajer, M. Paprzycka, Y.-X. Liu, A. M. Zagoskin, and F. Nori, State-dependent photon blockade via quantum-reservoir engineering, Phys. Rev. A **90**, 033831 (2014).

[75] M.-A. Lemonde, N. Didier, and A. A. Clerk, Antibunching and unconventional photon blockade with Gaussian squeezed states, Phys. Rev. A **90**, 063824 (2014).

[76] A. Miranowicz, M. Bartkowiak, X. Wang, Y.-X. Liu, and F. Nori, Testing nonclassicality in multimode fields: A unified derivation of classical inequalities, Phys. Rev. A **82**, 013824 (2010).

[77] M. Radulaski, K. A. Fischer, K. G. Lagoudakis, J. L. Zhang, and J. Vučković, Photon blockade in two-emitter-cavity systems, Phys. Rev. A **96**, 011801(R) (2017).

[78] J. Peřina Jr., V. Michálek, and O. Haderka, Higher-order sub-Poissonian-like nonclassical fields: Theoretical and experimental comparison, Phys. Rev. A **96**, 033852 (2017).

[79] J. Peřina Jr., V. Michálek, and O. Haderka, Simultaneous observation of higher-order non-classicalities based on experimental photocount moments and probabilities, Sci. Rep. **9**, 8961 (2019).

[80] G. S. Agarwal, Master Equation Methods in Quantum Optics, Prog. Opt. **11**, 1 (1973).

[81] J. Peřina, *Quantum Statistics of Linear and Nonlinear Optical Phenomena* (Kluwer, Dordrecht, 1991).

[82] M. O. Scully and M. S. Zubairy, *Quantum Optics* (Cambridge University, Cambridge, England, 1997).

[83] A. Lukš, V. Peřinová, and J. Peřina, Principal squeezing of vacuum fluctuations, Opt. Commun. **67**, 149 (1988).

[84] R. Loudon, Graphical representation of squeezed-state variances, Opt. Commun. **70**, 109 (1989).

[85] W. Vogel and D. Welsch, *Quantum Optics* (Wiley, New York, 2006).

[86] R. Loudon, *The Quantum Theory of Light* (Oxford University, London, 1973).

[87] C. T. Lee, Measure of the nonclassicality of nonclassical states, Phys. Rev. A **44**, R2775(R) (1991).

[88] M. Hillery, Nonclassical distance in quantum optics, Phys. Rev. A **35**, 725 (1987).

[89] A. Kenfack and K. Życzkowski, Negativity of the Wigner function as an indicator of non-classicality, J. Opt. B: Quantum Semicl. Opt. **6**, 396 (2004).

[90] A. Miranowicz, K. Bartkiewicz, A. Pathak, J. Peřina, Jr., Y.-N. Chen, and F. Nori, Statistical mixtures of states can be more quantum than their superpositions: Comparison of nonclassicality measures for single-qubit states, Phys. Rev. A **91**, 042309 (2015).

[91] J. K. Asbóth, J. Calsamiglia, and H. Ritsch, Computable Measure of Nonclassicality for Light, Phys. Rev. Lett. **94**, 173602 (2005).

[92] R. Horodecki, P. Horodecki, M. Horodecki, and K. Horodecki, Quantum entanglement, Rev. Mod. Phys. **81**, 865 (2009).

[93] A. Miranowicz, K. Bartkiewicz, N. Lambert, Y.-N. Chen, and F. Nori, Increasing relative nonclassicality quantified by standard entanglement potentials by dissipation and unbalanced beam splitting, Phys. Rev. A **92**, 062314 (2015).

[94] C. Eltschka and J. Siewert, Negativity as an Estimator of Entanglement Dimension, Phys. Rev. Lett. **111**, 100503 (2013).

[95] M. Bartkowiak, A. Miranowicz, X. Wang, Y.-X. Liu, W. Leoński, and F. Nori, Sudden vanishing and reappearance of nonclassical effects: General occurrence of finite-time decays and periodic vanishings of nonclassicality and entanglement witnesses, Phys. Rev. A **83**, 053814 (2011).

[96] I. I. Arkhipov, J. Peřina Jr., J. Svozilík, and A. Miranowicz, Nonclassicality invariant of general two-mode Gaussian states, Sci. Rep. **6**, 26523 (2016).

[97] N. Bartolo, F. Minganti, W. Casteels, and C. Ciuti, Exact steady state of a Kerr resonator with one- and two-photon driving and dissipation: Controllable Wigner-function multimodality and dissipative phase transitions, Phys. Rev. A **94**, 033841 (2016).

[98] F. Minganti, N. Bartolo, J. Lolli, W. Casteels, and C. Ciuti, Exact results for Schrödinger cats in driven-dissipative systems and their feedback control, Sc. Rep. **6**, 26987 (2016).

[99] J.-H. An, S.-J. Wang, H.-G. Luo, and C.-L. Jia, Production of squeezed state of single mode cavity field by the coupling of squeezed vacuum field reservoir in nonautonomous case, Chin. Phys. Lett. **21**, 1 (2004).

[100] H. Fearn and M. Collett, Representations of squeezed states with thermal noise, J. Mod. Opt. **35**, 553 (1988).